Regulation of cytoskeleton by small GTPase Rho and its targets

低分子量GTP結合蛋白質Rhoおよびその標的蛋白質による細胞骨格系の制御機構

天野　睦紀
奈良先端科学技術大学院大学
バイオサイエンス研究科
細胞生物学専攻
細胞内情報学講座
（貝淵弘三教授）

平成10年１月23日提出

SUMMARY

The small GTPase Rho is implicated in physiological functions associated with actin-myosin filaments such as cytokinesis, cell motility, cell adhesion and smooth muscle contraction. Three of proteins, serine-threonine kinase, protein kinase N (PKN), the myosin binding subunit (MBS) of myosin phosphatase, and newly identified serine-threonine kinase, Rho-associated protein kinase (Rho-kinase), were identified as Rho targets. The GTP-bound form of RhoA directly bound to and activated both PKN and Rho-kinase. Activated RhoA also formed a complex with the MBS. *In vitro*, Rho-kinase, which was activated by Rho, phosphorylated myosin light chain (MLC), thereby activating myosin ATPase. Rho-kinase also phosphorylated myosin phosphatase, leading to the inactivation of myosin phosphatase. Microinjection of constitutively active Rho-kinase in fibroblasts led to the formation of stress fibers and focal adhesions. Microinjection of dominant negative forms of Rho-kinase inhibited the lysophosphatidic acid (LPA)-induced stress fiber and focal adhesion formation. Thus, Rho-kinase appears to mediate signals from Rho and to induce the formation of stress fibers and focal adhesions, probably via specific substrates including MBS and MLC.

INTRODUCTION

The Rho family of proteins, like other GTPases, exhibit both GDP/GTP-binding and GTPase activities (1). They have the GDP-bound inactive and GTP-bound active forms which are interconvertible by GDP/GTP exchange and GTPase reactions (1). The GDP/GTP exchange reaction is regulated by stimulatory proteins such as Smg GDS (2,3), Dbl (4), Ost (5), and Tiam-1 (6) and by inhibitory proteins such as Rho GDI (7). The GTPase reaction is regulated by Rho GTPase-activating proteins (GAP) such as Ras GAP-associated p190 (8), Rho GAP (9), and Rho GAP p122 (10). Members of the Rho family of proteins, including RhoA, B, C, Rac1, 2 and Cdc42 share more than 50% sequence identity with each other (1). Rho is involved in appropriate responses of cytoskeletal network to extracellular signals such as lysophosphatidic acid (LPA) and certain growth factors to form stress fibers and focal adhesions (11,12). Rho is also involved in other physiological functions associated with cytoskeletal rearrangements such as cell morphology (13), cell aggregation (14), cell motility (15), and cytokinesis (16,17). Recent studies indicate that Rho is also involved in regulation of smooth muscle contraction (18), phosphatidylinositol 3-kinase (PI3-kinase) (19,20), phosphatidylinositol 4-phosphate 5-kinase (PI4,5-kinase) (21), and c-*fos* expression (22). Rac has been shown to be involved in the formation of membrane ruffling and

lamellipodia in fibroblasts (23,24). Cdc42 was originally identified in the yeast *Saccharomyces cerevisiae*, where it regulates polarized cell growth (25). Cdc42 regulates the formation of actin-containing microspike, called filopodia, in fibroblasts (26,27).

Upon stimulation with certain extracellular signals, the GDP-bound form of the Rho family of proteins may be converted to the GTP-bound form, and then they bind to specific targets and exert their biological functions (26). Cdc42 appears to be downstream from bradykinin, Rac appears to be downstream from PDGF and insulin, and Rho appears to be downstream from LPA (26,27). Recent studies demonstrate that in Swiss 3T3 cells, a cascade of Cdc42 controlling Rac controlling Rho coordinates the actin cytoskeleton during cell movement (26,27). For example, bradykinin appears to stimulate the cascade via Cdc42, producing the effects of Cdc42 activation (filopodia) followed by Rac activation (lamellipodia), and subsequent Rho activation (stress fibers and focal adhesions) (26,27).

The target molecules for Rac1 have been identified to be serine-threonine kinase PAK (28,29), WASP (30,31), IQGAP (32-35), and POR1 (36). Among these targets, POR1 has been shown to specifically interact with Rac1, but not with Cdc42. The other targets for Rac1 can interact with Cdc42. p85 subunit of PI3-kinase is also directly associated with

activated Rac and Cdc42 (37). However, the specific targets for Rho have not yet been identified.

In the present study, I identified putative targets for RhoA; protein kinase N (PKN) (38), novel serine-threonine kinase Rho-kinase (39), and the myosin binding subunit (MBS) of myosin phosphatase (40). I demonstrated that Rho-kinase phosphorylated MBS and consequently inactivated myosin phosphatase *in vitro* (40). Rho-kinase also phosphorylated myosin light chain (MLC) and thereby activated myosin ATPase (41). Constitutively active Rho-kinase could induce the formation of stress fibers and focal adhesions when injected into intact cells (42).

EXPERIMENTAL PROCEDURES

Materials and chemicals ———Glutathione *S*-transferase (GST)-RhoA, GST-RhoA^{A37}, GST-RhoA^{I41}, GST-Rac1, GST-H-Ras, GST-RB, GST-COIL, GST-PH, GST-MLC, GST-MLC^{A18A19}, GST-C3 transferase (C3), maltose binding protein (MBP)-PKN-N, MBP-MBS-N, and MBP-MBS-C were produced, and purified from *E. coli*. GST-CAT and GST-CAT-KD were produced in *Spodoptera frugiperda* cells (Sf9 cells) with a baculovirus system and purified on a glutathione-Sepharose column. pGEX-C3 was kindly provided by Dr. Hall, (University College of London). For microinjection, GST-C3 and GST-RhoA^{I41} were cleaved with thrombin, purified to remove the GST, and concentrated (43,23). MLC, Myosin and MLC kinase from the frozen chicken gizzard were kindly provided by Dr. Ito (Mie University School of Medicine). F-actin was purified from the rabbit skeletal muscle (44). LPA, anti-vinculin antibody, and tetramethyl rhodamine isothiocyanate (TRITC)-labeled phalloidin were purchased from Sigma Chemical Co. (St. Louis, MO, USA). Calyculin A was purchased from Wako Pure Chemical Industries (Osaka, Japan). [γ-^{32}P]ATP was purchased from Amersham Corp. All materials used in the nucleic acid study were purchased from Takara Shuzo Co. (Kyoto, Japan). Other materials and chemicals were obtained from commercial sources.

Plasmid constructs ———The cDNA fragment of RhoA^{I41} and MLC^{A18A19} were generated by the site-directed mutagenesis

and subcloned into pGEX-2T. pEF-BOS-HA-RhoA^{V14} was constructed as described (45). pEF-BOS-myc-CAT (amino acids 6 to 553), pEF-BOS-myc-CAT-KD (mutated at ATP-binding site; Lys^{121} to Gly), pEF-BOS-myc-COIL (amino acids 421 to 701), pEF-BOS-myc-RB (amino acids 941 to 1075), and pEF-BOS-myc-PH (amino acids 1125 to 1388) were constructed.

Affinity column chromatography ———The crude membrane fraction was prepared from bovine brain gray matter (200g) (46). The proteins of the membrane fraction were extracted by the addition of an equal volume of Homogenizing buffer [25 mM Tris-HCl (pH 7.5), 5 mM EGTA, 1 mM dithiothreitol (DTT), 10 mM $MgCl_2$, 10% sucrose] containing 4 M NaCl (100 ml), and the extract was dialyzed against Buffer A [20 mM Tris-HCl (pH 7.5), 1 mM EDTA, 1 mM DTT, 5 mM $MgCl_2$]. Solid ammonium sulfate was added to a final concentration of 40% saturation. The precipitate was dissolved in 16 ml of Buffer A and dialyzed against Buffer A and then passed over a 1-ml glutathione-Sepharose column. One eighth of the pass-through fraction (2 ml) was loaded onto a 0.25-ml glutathione-Sepharose column containing 6 nmol of respective small GTPases preloaded with guanine nucleotides as indicated. The columns were washed with 2.5 ml of Buffer A, and bound proteins were eluted with respective small GTPases by the addition of 0.825 ml of Buffer A containing 10 mM glutathione.

Cloning of the cDNA of Rho-kinase (p164) ———To obtain cDNA clones encoding Rho-kinase (p164), a bovine brain cDNA library (1.2 x 10^6 independent plaques in total) was screened with degenerate oligonucleotide probes according to the partial amino acid sequences determined from purified Rho-kinase (indicated by double underlines in Fig. 2). Hybridization for screening of the library was done as described (47). The cDNA inserted into λgt10 phage DNA was cloned into pBluescript II SK(-) (48) for nucleotide sequencing and into pEF-BOS-myc for expressing in mammalian cells.

Interaction of RhoA with recombinant PKN, Rho-kinase, and MBS in a cell-free system ———1) MBP-PKN-N (amino acids 7 to 155) (0.2 nmol) was mixed with glutathione-Sepharose beads (30 μl) containing 0.75 nmol of either GST, GDP·GST-RhoA, guanosine 5'-(3-*O*-thio)triphosphate (GTPγS)·GST-RhoA, GTPγS·GST-$RhoA^{A37}$, GDP·GST-Rac1, GTPγS·GST-Rac1, GDP·GST-H-Ras, or GTPγS·GST-H-Ras in 0.8 ml of Buffer A. MBP-PKN-N was eluted by the addition of 0.1 ml of Buffer A containing 0.2 M NaCl three times and then by the addition of 0.1 ml of Buffer A containing 10 mM glutathione three times. Portions (30 μl each) of the first fraction of the glutathione-eluate were subjected to SDS-PAGE followed by silver staining.

2) To obtain the *in vitro*-translated rat MBS (amino acids 1 to 976), pCRII-MBS was constructed. The MBS was translated

in vitro using the TNT T7 coupled reticulocyte lysate system (Promega) under the conditions described in the instruction manual. GST-small GTPases loaded with guanine nucleotides (0.75 nmol each) were immobilized onto 31 μl of glutathione-sepharose beads and washed with 310 μl (10 volumes) of Buffer A. The immobilized beads were added to 30 μl of *in vitro*-translated mixture and gently mixed for 1 h at 4°C in the presence of 1 mg/ml bovine serum albumin (BSA). The beads were washed six times with 102 μl (3.3 volumes) of Buffer A, and the bound proteins were eluted with GST-small G proteins by the addition of 102 μl (3.3 volumes) of Buffer A containing 10 mM glutathione three times. The first eluates were subjected to SDS-PAGE and vacuum-dried followed by autoradiography.

Overlay assay ———The method is a modified form of the one described previously (49). Briefly, the sample was applied to 6% SDS-PAGE and blotted to a nitrocellulose membrane. The membrane was incubated at 4°C for 5 min with Buffer B (25 mM Hepes/NaOH at pH 7.0, 0.5 mM $MgCl_2$, 0.05% Triton X-100) containing 6 M guanidium hydrochloride followed by incubation for 3 min with Buffer B. This was repeated four times and then an equal volume of Buffer B containing 6 M guanidium hydrochloride was added. The membrane was agitated for 10 min and an equal volume of Buffer B was added five times sequentially for 10 min each. The membrane was soaked in Buffer B, transferred into

phosphate buffer saline (PBS) containing 1% BSA, 0.1% Triton X-100, 0.5 mM $MgCl_2$, and 5 mM DTT, then immersed for 10 min with 0.5 ml of GAP buffer (25 mM Hepes/NaOH at pH 7.0, 2.5 mM DTT, 5 mM $MgCl_2$, 0.05% Triton X-100, 100 mM GTP) containing [^{35}S]GTPγS·GST-RhoA or [^{35}S]GTPγS·GST-RhoA^{A37}. The membrane was washed three times with PBS containing 25 mM Hepes/NaOH at pH 7.0, 5 mM $MgCl_2$, and 0.05% Triton X-100, dried and exposed to an X-ray film.

Protein kinase assay ———The kinase reaction for PKN and Rho-kinase was carried out in 50 µl of kinase buffer [50 mM Tris/HCl at pH 7.5, 1 mM EDTA, 1 mM DTT, 5 mM $MgCl_2$, 0-0.15% 3-[(3-Cholamidopropyl) dimethylammonio] propanesulfonic acid (CHAPS)] containing 2-250 µM [γ-^{32}P]ATP (10-800 GBq/mmol) and purified PKN, Rho-kinase or GST-CAT. The kinase reaction for MLC kinase was carried out in 50 µl of the reaction mixture (50 mM Tris/HCl at pH 7.5, 1 mM $MgCl_2$, 85 mM KCl, 250 µM [γ-^{32}P]ATP [0.5-5 GBq/mmol], purified enzyme and indicated amounts of MLC or myosin) with or without 0.1 mM $CaCl_2$ and 10 µg/ml calmodulin. After an incubation for 10 min at 30°C, the reaction mixtures were boiled in SDS-sample buffer and resolved by SDS-PAGE. The radiolabeled bands were visualized by autoradiography or by Fuji image analyzer BAS-2000. To examine the phosphorylation of S6 peptide, αPKC peptide, and myelin basic protein, the reaction mixtures were spotted onto

Whatman p81 paper. The incorporation of ^{32}P into the substrates was assessed by scintillation counting.

Thiophosphorylation of myosin phosphatase and MLC phosphatase assay ———Thiophosphorylation of myosin phosphatase (1 μg of protein) was carried out in 50 μl of kinase buffer in the presence of 10 μM [^{35}S]adenosine 5'-(3-*O*-thio)-triphosphate (ATPγS) (8-10 GBq/mmol) instead of [γ-^{32}P]ATP. After an incubation for 6 min at 30°C, 40 μl of the reaction mixtures were subjected to SDS-PAGE and 10 μl of the reaction mixtures were used for the MLC phosphatase assay. The MLC phosphatase activity was assayed for 6 min at 30°C in 50 μl of reaction mixture (30 mM Tris/HCl at pH 7.5, 30 mM KCl, 3 mM $MgCl_2$, 5 mM EDTA, 1 mM DTT, 5 μM ^{32}P-MLC and samples) (50).

Detection of phosphorylation of MBS in NIH 3T3 cell lines ———NIH 3T3 cells were stably transfected with p3'SS and pOPRSVI-HA-RhoA or pOPRSVI-HA-$RhoA^{V14}$ to establish NIH 3T3 cell lines overexpressing RhoA or $RhoA^{V14}$ under the control of isopropyl-β-D-thiogalactopyranoside (IPTG) according to the manufactural instruction (Stratagene). Confluent NIH 3T3 cell lines (the parent cells, NIH 3T3-RhoA-5, NIH 3T3-RhoA-24, NIH 3T3-$RhoA^{V14}$-7, and NIH 3T3-$RhoA^{V14}$-24) (35 mm dish) were treated with 5 mM IPTG for 24 h. During the last 12 h, the cells were serum-starved, and then labeled with 9.25 MBq of [^{32}P]-orthophosphate for 2 h. The ^{32}P-labeled cells were then lysed, and MBS was

immunoprecipitated. The washed immunoprecipitates were subjected to SDS-PAGE for autoradiography. Stimulation fold of MBS phosphorylation was calculated by image analyzer.

Detection of phosphorylation of MLC in NIH 3T3 cell lines ———IPTG-treated and serum-starved NIH 3T3 cell lines (100 mm dish) were added with 10% trichloroacetic acid (TCA). To determine the extent of MLC phosphorylation, the TCA precipitable materials were subjected to glycerol-urea gel electrophoresis followed by quantitation of the relative amounts of non-phosphorylated and phosphorylated forms of MLC with immunoblot technique (51). To examine the effect of calyculin-A, NIH 3T3 cells were treated with 0.1 μM calyculin-A for 10 min.

Myosin ATPase assay ———Myosin ATPase assay was carried out as described (52) with minor modifications. Briefly, 0.1 mg/ml myosin was phosphorylated by GST-CAT (450 ng of protein) in 0.45 ml of the reaction mixture (50 mM Tris/HCl at pH 7.5, 1 mM DTT, 5 mM $MgCl_2$, 1 mM EGTA, 85 mM KCl and 500 μM ATP [80-200 MBq/mmol]) for 20 min at 30°C. Myosin was phosphorylated by MLC kinase (450 ng of protein) under the similar conditions except in the presence of 0.1 mM $CaCl_2$ and 10 μg/ml calmodulin. The myosin ATPase reaction was carried out in 0.1 ml of ATPase buffer (0.05 mg/ml phosphorylated myosin, 50 mM Tris/HCl at pH 7.5, 0.5 mM DTT, 10 mM $MgCl_2$, 0.5 mM EGTA, 85 mM KCl, and 1 mM ATP [80-200 MBq/mmol]) at the indicated concentrations of F-actin for 30

min at 30°C. An aliquot (80 µl) of the reaction mixture was added into the stop solution (1.3% charcoal, 0.12 M NaH_2PO_4 and 0.33 M perchloric acid) and filtrated. Inorganic phosphate that was liberated from [γ-^{32}P]ATP was assessed by a scintillation counter.

Microinjection and immunofluorescense analysis —Swiss 3T3 cells were cultured in Dulbecco's modified Eagle's medium (DMEM) supplemented with fetal bovine serum (10%). Cells were seeded at a density of 8-10 x 10^3 cells onto 12 mm glass coverslips. After 4 days, the cells were deprived of serum for 24 h in DMEM. Recombinant proteins were microinjected along with a marker protein (rabbit IgG, 1 mg/ml) into the cytoplasm of cells. After microinjection, the cells were incubated at 37°C for 30 min. Actin and vinculin were visualized by TRITC-labeled phalloidin and an antibody to vinculin, respectively, as described (11,12). Nuclei were visualized by bis-benzimide.

Other Procedures ———SDS-PAGE was performed as described, previously (53). A phosphopeptide mapping analysis of MLC was carried out as described (54). A phosphoamino acid analysis of MLC was carried out as described (55). The immunoblot analysis was carried out as described (56).

RESULTS

Purification and identification of Rho-interacting proteins

To enrich RhoA-interacting proteins, crude extracts of a bovine brain membrane fraction were fractionated by the addition of ammonium sulfate (40%). The precipitated proteins were loaded onto one of four glutathione-Sepharose affinity columns on which GST, GDP·GST-RhoA, GTPγS (a nonhydrolyzable GTP analog)·GST-RhoA, or GTPγS·GST-RhoA^{A37} (which contains an amino acid substitution in the effector domain) recombinant proteins were immobilized. Proteins bound to the affinity columns were then eluted with GST-RhoA by the addition of glutathione (Fig. 1). At lease four proteins with molecular masses of 128 kDa, 138 kDa, 164 kDa, and 180 kDa (named p128, p138, p164, and p180, respectively) were identified in the eluate from the GTPγS·GST-RhoA affinity column but not from the GST or GDP·GST-RhoA affinity columns, indicating that these proteins specifically interacted either directly or indirectly with the GTPγS·GST-RhoA. These proteins appeared to show weaker affinity for the effector domain mutant, GST-RhoA^{A37}, because less amounts of these proteins were retained on the GTPγS·GST-RhoA^{A37} affinity column than that for GTPγS·GST-RhoA. The specificity was further examined on affinity column chromatography with GST-Rac1 and GST-H-Ras as probes. Three proteins of 122 kDa, 140 kDa, and 182 kDa, distinct

from the above RhoA-interacting proteins, were eluted from the GTPγS·GST-Rac1 affinity column but not from the GDP·GST-Rac1 affinity column (Fig. 1). I confirmed that the 140 kDa and 182 kDa Rac1-interacting protein were distinguishable from p138 and p180 by electrophoresis, respectively. Neither p128, p138, p164, nor p180 was eluted from the GTPγS·GST-H-Ras affinity column. I conclude that the four proteins p128, p138, p164, and p180 interact specifically with activated RhoA.

Among the RhoA-interacting proteins identified, I enriched p128 by specific elution from the GTPγS·GST-RhoA affinity column in the presence of 0.2 M NaCl (data not shown). The p128 protein was further purified to near homogeneity (greater than 95%) by DEAE Sepharose column chromatography. Purified p128 was subjected to amino acid sequencing. Five peptide sequences derived from p128 were determined. These were QLAIELK, NVLRLL, LGLLREALERRL, SPLTLEDF, and VLLSEFRP. They were found within the sequence of the human serine-threonine kinase PKN/PRK1 (57,58), which has an apparent molecular size of 120 kDa on SDS-PAGE, close to that of p128. Immunoblot analysis demonstrated that p128 was recognized by antibody to PKN (data not shown). I therefore conclude that p128 is the bovine PKN.

Nine peptide sequences derived from p138 were determined: RWIGSE, SLLQM, GYTEVL, ETLIIEPEK, DESPA, AYVAPTV, SLQGI, AQLHDTNMAL, and DENGALIRVIS. They were

almost identical to those of rat 110-kDa regulatory subunit of smooth muscle protein phosphatase 1M (50), which is a rat homologue of the myosin-binding subunit (MBS) of myosin phosphatase form chicken (59). I further confirmed that p138 is the MBS by immunoblot analysis. The p138 protein was recognized by antibody to MBS, and an immunoreactive band was specifically detected in the eluate from the GTPγS·GST-RhoA affinity column (data not shown). Therefore, I concluded that p138 is a bovine counterpart of MBS. I hereafter refer to it as MBS. Myosin phosphatase is composed of the MBS, a 37-kDa type 1 phosphatase catalytic subunit, and a 20-kDa regulatory subunit (50,59). I examined whether the other subunits were retained on the GTPγS·GST-RhoA affinity column. An immunoreactive band corresponding to catalytic subunit was specifically detected in the eluate from the GTPγS·GST-RhoA affinity column (data not shown). An immunoreactive band corresponding to the 20-kDa regulatory subunit was detected in the membrane extract, but not detected in any of the eluates, suggesting that interaction of RhoA with myosin phosphatase may cause dissociation of the 20-kDa regulatory subunit from the holoenzyme. Alternatively, RhoA may interact specifically with myosin phosphatase composed of MBS and the catalytic subunit. MLC phosphatase activity was specifically detected in the eluate from the GTPγS·GST-RhoA affinity column (data not shown).

I next enriched p164 through specific elution from the GTPγS·GST-RhoA affinity column in the presence of 1% CHAPS (data not shown). To further purify p164, the partially purified p164 was subjected to Mono Q column chromatography. p164 appeared as a single peak in the column chromatography and was purified to near homogeneity (greater than 95%) (data not shown), and purified protein was subjected to amino acid sequencing. Thirty seven peptide sequences derived from p164 were determined, and revealed that it was novel protein.

Isolation of the p164 cDNA

To clarify a molecular identity of p164, two sequences of the peptides were used to design the degenerate oligonucleotide probes for the cDNA cloning. By use of degenerate oligonucleotide probes, the cDNA encoding the complete sequence of p164 was isolated from a bovine cDNA library. The predicted protein contains 1388 amino acid residues with a calculated molecular mass of 160,739 Da, which is close to its apparent Mr, 164 kDa, estimated by SDS-PAGE (Fig. 1). The deduced amino acid sequence is shown in Fig. 2. All thirty seven peptide sequences obtained were found within the deduced amino acid sequence. The neighboring sequence around the initiation codon was consistent with the translation initiation start site proposed by Kozak (60) and I found a in-frame termination codon in the preceding region. The predicted protein

product has the putative kinase domain in the N-terminal portion and it shares 72% sequence homology with myotonic dystrophy kinase within the kinase domain (Fig. 3) (61-63).. p164 has a putative coiled-coil structure which shows a significant similarity with myosin rod in the middle portion, and a pleckstrin-homology (PH) domain in the C-terminal portion. On the basis of these results, I hereafter designated p164 as Rho-associated kinase (Rho-kinase).

Specific interaction of PKN, MBS, and Rho-kinase with RhoA

To address whether PKN, MBS, and Rho-kinase are the target proteins of Rho, specific interaction between recombinant proteins of them and GTPγS·RhoA was investigated.

Because PKN is composed of an NH_2-terminal regulatory domain and a COOH-terminal catalytic domain (57,58), I tested whether RhoA directly binds the NH_2-terminal domain of PKN. The NH_2-terminal domain of PKN (amino acids 7 to 155) was expressed as a MBP fusion protein and mixed with beads coated with GST-RhoA. The MBP-PKN-N fusion protein was retained on the GTPγS·GST-RhoA beads and could be eluted by 0.2 M NaCl and eluted with GTPγS·GST-RhoA by the addition of glutathione (Fig. 4). The fusion protein was not retained on beads coated with GST, GDP·GST-RhoA, GTPγS·GST-$RhoA^{A37}$, GTPγS·GST-Rac1, or GTPγS·GST-H-Ras. Scatchard

analysis indicated that MBP-PKN-N formed a 1:1 complex with GTPγS·GST-RhoA. The apparent *Kd* value for MBP-PKN-N was estimated to be about 0.4 μM.

To examine the direct binding of GTPγS·GST-RhoA to Rho-kinase, the overlay assay with [^{35}S]GTPγS·GST-RhoA was carried out. [^{35}S]GTPγS·GST-RhoA bound to Rho-kinase in the membrane extract and purified preparation, whereas [^{35}S]GTPγS·GST-RhoA^{A37} did not bind to it (Fig. 5), indicating that activated RhoA directly binds to native Rho-kinase via the effector domain. [^{35}S]GTPγS·GST-Rac1 did not bind to Rho-kinase (data not shown). To determine the Rho-binding domain of Rho-kinase, I divided Rho-kinase into several fragments and expressed as GST-fusion proteins in *E. coli*. Among these fragments of Rho-kinase, the COOH-terminal of coiled coil domain (amino acids 941 to 1075) specifically bound GTPγS·RhoA, but not GTPγS·RhoA^{A37} in the overlay assay (data not shown). I concluded that activated RhoA directly interacts with this region of Rho-kinase, and refereed to the region as Rho-binding (RB) domain.

The *in vitro*-translated MBS was also mixed with the affinity beads coated with GST-RhoA, and MBS was retained on the affinity beads coated with GTPγS·GST-RhoA and eluted with GTPγS·GST-RhoA by the addition of glutathione (data not shown). I confirmed that the COOH-terminal domain of MBS (amino acids 699 to 976) interacted with dominant activated RhoA (RhoA^{V14}) but not with RhoA in a yeast two-hybrid

system (data not shown). $RhoA^{V14}$ is structurally equivalent to $H\text{-}Ras^{V12}$ (1,64). Because $RhoA^{V14}$ has decreased GTPase activity and is insensitive to Rho GAP, it exists mainly in a GTP-bound form in intact cells (11-13). The NH_2-terminal domain of MBS (amino acids 1 to 707) interacted weakly with $RhoA^{V14}$ but not with RhoA. The COOH-terminal domain of MBS contains a polybasic region followed by a leucine zipper-like motif (50). Because PKN also has similar polybasic region followed by a leucine zipper-like motif in the region where it interacts with Rho, this may represent consensus motif for interaction with Rho. On the other hand, I do not find any sequence similarity between the NH_2-terminal domain of MBS and the Rho-interacting sites of PKN and Rho-kinase.

Regulation of the kinase activity of PKN and Rho-kinase by RhoA

I further tested whether GTP·RhoA could act as a modulator of PKN and Rho-kinase kinase activity.

Purified PKN phosphorylates exogenous substrates such as myelin basic protein and serine-containing synthetic peptides based on the pseudosubstrate site of protein kinase C (PKC) (which corresponds to amino acids 19 to 35 of bovine PKCα, except that Ser is substituted for Ala; RFARKGSLRQKNVHEVK). GTPγS·GST-RhoA stimulated PKN kinase activity in a dose-dependent manner, whereas GDP·GST-RhoA

was ineffective (Fig. 6). GTPγS·GST-Rac1 showed only a small effect and GTPγS·GST-H-Ras had no effect (Fig. 6).

I then examined the kinase activity of Rho-kinase toward exogenous substrates such as S6 peptide. Rho-kinase phosphorylated S6 peptide and GTPγS·GST-RhoA stimulated this reaction, whereas GDP·GST-RhoA had a much weaker effect. I also examined phosphorylation of αPKC peptide and myelin basic protein, and found that GTPγS·GST-RhoA was able to stimulate the kinase activity toward PKCα peptide and myelin basic protein. Among these substrates, S6 peptide was the most preferable substrate for Rho-kinase (data not shown). I next examined the effect of various small GTP-binding proteins on the kinase activity of Rho-kinase and found that GTPγS·GST-RhoA^{A37} and GTPγS·GST-Rac1 showed only a residual effect and GTPγS·GST-H-Ras had no effect (data not shown). Since Rho is implicated in cytoskeletal rearrangements, I searched for substrates for Rho-kinase among cytoskeletal regulatory proteins including vinculin, talin, metavinculin, caldesmon, filamin, vimentin, α-actinin (65), MAP-4 (66), and MBS of myosin phosphatase (59,50). Among them, MBS is the most preferable substrate for Rho-kinase. GTPγS·GST-RhoA stimulated the kinase activity toward MBS about 15 fold (Fig. 7).

Regulation of the myosin phosphatase activity by Rho-kinase

I examined whether GTPγS·GST-RhoA modulates the activity of myosin phosphatase, and found that GTPγS·GST-RhoA did not modulate the activity of MLC phosphatase (data not shown). It has been shown that thiophosphorylation of MBS is associated with inhibition of the myosin phosphatase activity in permeabilized smooth muscles (67). These observations prompted us to examine whether PKN and Rho-kinase phosphorylate MBS. Rho-kinase phosphorylated the COOH-terminal domain of MBS (amino acids 753 to 1004) (MBS-C) (Fig. 7) but did not phosphorylate the NH_2-terminal domain of MBS (amino acids 1 to 721) (MBS-N), whereas PKN hardly phosphorylated either fragment (data not shown). GTPγS·GST-RhoA stimulated the kinase activity of Rho-kinase toward MBS-C, but GDP·GST-RhoA (Fig. 7), GTPγS·GST-$RhoA^{A37}$ or GTPγS·GST-Rac1 (data not shown) did not. To examine whether Rho-kinase regulates the MLC phosphatase activity through the phosphorylation of MBS, I tested whether Rho-kinase thiophosphorylates the native holoenzyme in the presence of ATPγS. The holoenzyme has phosphatase activity toward itself, so I measured thiophosphorylation, which is resistant to phosphatase activity (67). The MBS of the holoenzyme was slightly thiophosphorylated in the absence of Rho-kinase, presumably because of its contamination with an unidentified kinase. Rho-kinase thiophosphorylated MBS in a dose-dependent manner (Fig. 8). Thiophosphorylation of MBS was associated with a decrease in the MLC phosphatase

activity (Fig. 8). The decrease of the MLC phosphatase activity depended on the simultaneous presence of ATPγS and Rho-kinase. GTPγS·GST-RhoA enhanced both the thiophosphorylation and the inhibition of the phosphatase activity by Rho-kinase.

To test whether activated RhoA can stimulate the phosphorylation of MBS in intact cells, I established NIH 3T3 cell lines that expressed RhoA (RhoA-5, RhoA-24) or $RhoA^{V14}$ ($RhoA^{V14}$-7, $RhoA^{V14}$-25) under the control of an inducible promoter. Treatment of the cell lines with an inducer, IPTG stimulated RhoA or $RhoA^{V14}$ expression 2 to 5.4 fold depending on the cell lines, though they showed basal expression of RhoA or $RhoA^{V14}$. In these cell lines, large amounts of stress fibers and focal adhesions were observed in the presence or absence of IPTG (data not shown). The amounts of phosphorylation of MBS in the RhoA-5, RhoA-24, $RhoA^{V14}$-7 and $RhoA^{V14}$-25 cell lines was significantly greater than that in the parent NIH 3T3 cells when the cells were grown in the presence of IPTG, whereas phosphorylation of other major proteins (data not shown) and amounts of MBS (Fig. 9) were similar among these cell lines. Treatment of the $RhoA^{V14}$-7 cell line with IPTG stimulated expression of $RhoA^{V14}$ 5.4 ± 0.5 fold and increased MBS phosphorylation 2.0 ± 0.3 fold (data not shown). IPTG did not affect MBS phosphorylation in the parent NIH 3T3 cells and caused only slight increments of MBS phosphorylation in the RhoA-5,

RhoA-24 and RhoA^{V14}-25 cell lines, though IPTG did increase RhoA or RhoA^{V14} expression about 2 to 2.5 fold in the RhoA-5, RhoA-24 and RhoA^{V14}-25 cell lines. But the basal expression of RhoA or RhoA^{V14} in these cell lines may be sufficient to induce MBS phosphorylation. Thus, it is likely that Rho-kinase phosphorylates MBS in NIH 3T3 cells in a Rho-dependent fashion, though I can not exclude the possibility that other kinases are responsible for MBS phosphorylation.

Treatment of the parent NIH 3T3 cells with calyculin-A (a phosphatase inhibitor) increased phosphorylation of MLC (Fig. 10). The extent of phosphorylation of MLC in the RhoA-24 and RhoA^{V14}-7 cell lines in the presence of IPTG was greater than that in the parental NIH 3T3 cells (Fig. 10). Essentially identical results were obtained when the RhoA-5 and RhoA^{V14}-25 cell lines were used (data not shown).

Phosphorylation of MLC by Rho-kinase

I further examined whether Rho-kinase phosphorylates MLC directly in a cell-free system, and found that Rho-kinase phosphorylated MLC (Fig. 11). GTPγS·GST-RhoA enhanced the phosphorylation of MLC by Rho-kinase, but GDP·GST-RhoA or GTPγS·GST-RhoA^{A37} did not (Fig. 11). GTPγS·GST-Rac1 had no effect. Under the similar conditions, MLC kinase phosphorylated MLC in a Ca^{2+}-calmodulin-dependent manner (Fig. 11). I also found that Rho-kinase

phosphorylated the MLC of intact myosin in a GTPγS·GST-RhoA-dependent manner (Fig. 11).

About 1 mol of phosphate could be maximally incorporated into 1 mol of isolated MLC or MLC of intact myosin by Rho-kinase in the presence of GTPγS·GST-RhoA (data not shown). It is noted that a limited number of kinases such as MLC kinase and PKC are known to phosphorylate intact myosin stoichiometrically (68).

The apparent affinity of isolated MLC for Rho-kinase was estimated by measuring the phosphorylation of various concentrations of MLC (Fig. 12). The apparent K_m values for MLC in the presence and absence of GTPγS·GST-RhoA were 2.6 ± 0.4 and 12.6 ± 1.6 μM, and the molecular activities were 15.8 ± 2.0 and 9.0 ± 1.2 mol min^{-1} mol^{-1}, respectively. Thus, it is likely that GTPγS·GST-RhoA increases the affinity of Rho-kinase for MLC and produces the maximum velocity of the phosphorylation reaction. The apparent *K*m value and molecular activity of MLC kinase for MLC were 52.1 ± 7.1 μM and 120 ± 21.3 mol min^{-1} mol^{-1}, respectively, under the conditions (data not shown). The *K*m value of Rho-kinase for MLC was lower than that of MLC kinase, indicating that Rho-kinase phosphorylates myosin at lower concentrations, but the molecular activity of Rho-kinase was lower than that of MLC kinase.

MLC is phosphorylated primarily at Ser-19 and secondarily at Thr-18 by MLC kinase (69), and the

phosphorylation of Ser-19 is essential to facilitate actin-activation of myosin ATPase (70,71). MLC is phosphorylated at Ser-1, Ser-2 and Thr-9 by PKC, and this phosphorylation by PKC inhibits the actin-activation of myosin ATPase (72-74). To determine the primary phosphorylation site of MLC by Rho-kinase, I performed peptide mapping of the phosphorylated MLC by either Rho-kinase, MLC kinase or PKC *in vitro*. The phosphorylated MLC was digested with trypsin and the resulting peptides were separated by electrophoresis and chromatography. The pattern of two-dimensional peptide mapping of MLC phosphorylated by Rho-kinase was identical to that produced by MLC kinase, and different from that produced by PKC (Fig. 13). A phosphoamino acid analysis revealed that phosphorylation occurred mainly on the serine residue and partially on the threonine residue of the MLC that was phosphorylated by Rho-kinase, and that the phosphorylation occurred only on the serine residue of the MLC that was phosphorylated by the MLC kinase (data not shown). It may be noted that the MLC kinase preferentially phosphorylates MLC at Ser-19 in these conditions. I fused GST proteins with wild type MLC and with MLC containing a substitution for the alanine residues for Thr-18 and Ser-19. Then, I examined if Rho-kinase and MLC kinase could phosphorylate these recombinant proteins. Both Rho-kinase and MLC kinase phosphorylated GST-MLC but did not phosphorylate GST or GST-MLC^{A18A19}. PKC phosphorylated both

GST-MLC and GST-MLC^{A18A19} (data not shown). These results indicate that Rho-kinase phosphorylates MLC mainly at Ser-19, which is the same site phosphorylated by MLC kinase.

To examine whether Rho-kinase functions equivalently to MLC kinase in a cell-free system, I performed the actin-activated MgATPase assay. Purified intact myosin was phosphorylated to 1 mol/mol by GST-CAT (constitutively active from of Rho-kinase; discussed below), then the actin-activated MgATPase activity was measured. The MgATPase activity of the phosphorylated myosin increased in a F-actin-dependent manner to the extent similar to that increased by MLC kinase (Fig. 14). The apparent *Ka* values for actin and the molecular activity of the phosphorylated myosin were 0.56 ± 0.05 μM and 0.18 ± 0.02 sec^{-1}, respectively. These values were roughly the same as those for the myosin phosphorylated by MLC kinase. I used GST-Rho-kinase instead of native Rho-kinase in this experiment because high concentrations of myosin were necessary to detect the myosin ATPase activity and the stoichiometrical phosphorylation of myosin by native Rho-kinase was difficult under the conditions.

Expression of Rho-kinase and its mutants

To elucidate the functions of Rho-kinase among these targets of Rho, I produced dominant active and negative forms of Rho-kinase. Serine-threonine kinases such as PKC and Raf are usually composed of the regulatory and catalytic

domains (75-77). Deletion of the regulatory domains make PKC and Raf constitutively active, and the regulatory fragments serve as dominant negative forms of the kinases (78,79). Rho-kinase is composed of catalytic, coiled coil, Rho-binding, and pleckstrin-homology domains. I produced four fragments containing respective domains as GST-fusion proteins. GTPγS·GST-RhoA bound to Rho-binding domain (GST-RB, amino acids 941 to 1075), but GTPγS·GST-RhoA^{A37} bound to it very weakly (data not shown). Rho-kinase had kinase activity on MLC that was activated by GTPγS·GST-RhoA, whereas the catalytic domain (GST-CAT, amino acids 6 to 553) showed full kinase activity without addition of GTPγS·GST-RhoA (Fig. 15). The molecular activities of Rho-kinase in the presence of GTPγS·GST-RhoA and GST-CAT in the absence of GTPγS·GST-RhoA were 0.32 ± 0.02 s^{-1} and 0.71 ± 0.02 s^{-1}, respectively, indicating that GST-CAT is constitutively active. GST-CAT mutated at the ATP-binding site (GST-CAT-KD) did not have kinase activity. GST-RB inhibited GTPγS·GST-RhoA-stimulated Rho-kinase activity in a dose-dependent manner, whereas it did not affect kinase activity of GST-CAT (Fig. 16). Neither GST-CAT-KD, the coiled-coil domain (GST-COIL, amino acids 421 to 701), nor the pleckstrin-homology domain (GST-PH, amino acids 1125 to 1388) affected kinase activity of Rho-kinase. Neither GST-CAT-KD, GST-COIL, GST-RB, nor GST-PH inhibited kinase activity of PKN and MLC kinase (data not shown). Rho-

induced formation of stress fibers is inhibited by protein kinase inhibitors such as staurosporine (26,80). Staurosporine inhibited kinase activity of both Rho-kinase and GST-CAT (Fig. 16).

Confluent, serum-starved Swiss 3T3 cells had very few stress fibers, which were visualized by phalloidin (Fig. 17) as described (11,12). When the cells were stimulated with LPA, new stress fibers appeared and increased in number and diameter (Fig. 17) (11,12). Microinjection of GST-CAT also induced stress fiber formation (Fig. 17), whereas GST-CAT-KD was inactive in this capacity (data not shown). Injected GST-CAT often caused the formation of a large aggregate of actin filaments connected with stress fibers at the central area. When the cells were microinjected with C3, which ADP-ribosylates and inhibits Rho (81,82), the cells rounded up within 30 min (13). Injected C3 abolished the LPA-induced stress fiber formation (Fig. 17), whereas it did not inhibit GST-CAT-induced stress fiber formation. Coinjection of GST-CAT with C3 prevented the cells from rounding up. Cells stimulated by LPA in the presence of staurosporine showed randomly arranged actin filaments (Fig. 17) (26,80), but cells injected with GST-CAT in the presence of staurosporine did not form stress fibers.

Very few focal adhesions, visualized by an antibody to vinculin, were observed in confluent, serum-starved Swiss 3T3 cells (Fig. 18) (11,12). When the cells were stimulated

with LPA, new focal adhesions appeared and increased in number (11,12). Microinjection of GST-CAT induced focal adhesion formation. Longitudinal stress fibers newly synthesized after injection of GST-CAT were linked to elongated, arrowhead shape of focal adhesions as revealed by dual immunofluorescence analysis (Fig. 18). Thus it seems clear that GST-CAT-induced focal adhesions exhibit the specific features of adhesions elicited by Rho (26,80). Microinjection of C3 abolished the LPA-induced formation of focal adhesions, whereas it did not that induced by GST-CAT. Staurosporine inhibited both the LPA- and GST-CAT-induced formation of focal adhesions. Injection of constitutively active PKN or MBS did not induce formation of stress fibers and focal adhesions, or affect that induced by GST-CAT (data not shown).

Injection of GST-RB or GST-PH inhibited the LPA-induced formation of stress fibers and focal adhesions (Fig. 19). About 30% of the cells injected with GST-CAT-KD did not form stress fibers or focal adhesions in the presence of LPA. GST-COIL had no effects (Fig. 19). Injection of neither GST-CAT-KD, GST-COIL, GST-RB, nor GST-PH inhibited the GST-CAT-induced formation of stress fibers and focal adhesions, indicating that GST-CAT-KD, GST-RB, and GST-PH inhibited the functions of endogenous Rho-kinase but did not those of the exogenously overexpressed GST-CAT (data not shown).

Because Swiss 3T3 cells are not suitable for nuclear injection of plasmids, I examined the morphological effects of Rho-kinase in Madin-Darby canine kidney (MDCK) cells microinjected with the cDNAs encoding various domains of Rho-kinase. Microinjection of the cDNA encoding $RhoA^{V14}$ into MDCK cells resulted in increased formation of stress fibers and focal adhesions (data not shown). Stress fibers and focal adhesions formed in cells injected with the cDNA encoding CAT (data not shown). The cDNAs encoding CAT-KD, the constitutively active form of PKN, or MBS had no effect. Coinjection of the cDNAs encoding either CAT-KD, RB, or PH inhibited $RhoA^{V14}$-induced stress fiber formation (data not shown) and focal adhesion formation. CAT-KD was less effective than RB or PH. COIL was inactive in this capacity.

DISCUSSION

Target protein of Rho

Here, I identified at least three RhoA-interacting molecules; PKN, MBS, and Rho-kinase. I also demonstrated that activated RhoA binds them directly and modulates their enzymatic activity directly or indirectly, indicating these molecules are putative target proteins of Rho.

PKN is composed of an NH_2-terminal regulatory domain and a COOH-terminal catalytic domain (57,58). Although the catalytic domain of PKN is highly related to that of PKC, the NH_2-terminal domain is distinct from those of other protein kinases. The physiological functions of PKN are not known and further studies are necessary for better understanding the functions of the Rho-PKN pathway.

MBS is the myosin binding subunit of myosin phosphatase, which is composed of the MBS, catalytic subunit, and 20-kDa regulatory subunit (59,50). Although the definitive function of MBS has not yet been clarified, it appears to enhance the phosphatase activity of the catalytic subunit toward myosin by directly binding to phosphorylated myosin (83,84). As shown above, the dimeric myosin phosphatase composed of MBS and catalytic subunit interacts with activated RhoA, but the trimeric myosin phosphatase composed of MBS, catalytic subunit, and 20-kDa regulatory subunit does not. Although the role of 20-kDa

subunit is unclear, the dimeric myosin phosphatase shows the phosphatase activity towards MLC in vitro.

The third molecule interacting with Rho is novel serine-threonine kinase, named Rho-kinase. The NH_2-terminal catalytic domain of Rho-kinase is highly homologous to that of myotonic dystrophy kinase, which is the product of the gene that causes myotonic dystrophy (61-63). Myotonic dystrophy is an autosomal dominant multisystem disease that is characterized by muscle weakness, atrophy and myotonia (85). Although the catalytic properties of myotonic dystrophy kinase have not been compared with Rho-kinase, they may share similar catalytic properties. Furthermore, myotonic dystrophy kinase has a molecular design similar to Rho-kinase, except for the transmembrane domain (Fig. 3). The COOH-terminal region of Rho-kinase has the sequence conserved with PH domain, which is supposed to localize molecules at the specified regions.

Another groups of investigators also identified PKN (86), Rho-kinase/ROK (87), and $p160^{ROCK}$ (88), which is an isoform of Rho-kinase, as Rho-interacting molecules. Recently, additional target proteins of Rho, including rhophilin, rhotekin, and mDia has been reported (86,89,90). Taken together, upon stimulation, activated Rho seems to interact with the unique subsets of proteins and modulate their functions. This may account for distinct mechanisms

by which diversity is generated in downstream pathways for Rho-induced multiple cellular responses.

Interface between activated RhoA and its targets

I have identified the Rho-binding region of each molecule. RhoA interacts with the NH_2-terminal portion of PKN and with COOH-terminal half of MBS, both of which contain a polybasic region followed by a leucine zipper-like motif. The interface of the RhoA interaction has been localized to the COOH-terminal potion of coiled coil domain of Rho-kinase. There is no obvious sequence homology between the Rho-binding domain of Rho-kinase and that of PKN or MBS, suggesting that activated RhoA can recognize at least two different types of target interfaces.

Dual regulation of the level of MLC phosphorylation

The functions of kinases are defined by their physiological substrates. Rho-kinase phosphorylates MBS and consequently inactivates myosin phosphatase. Rho-kinase phosphorylates MLC of intact myosin and thereby activates myosin ATPase. MLC phosphorylation is essential for the actin-myosin interaction and thus actin-activated myosin ATPase (68,91-93). Rho-kinase may tightly regulate the level of myosin phosphorylation by dual pathways, and be involved in the acto-myosin reorganization downstream of Rho (Fig. 20).

When smooth muscles are stimulated by an agonist, Ca^{2+} is mobilized into the cytoplasm, which activates the

calmodulin-dependent MLC kinase. Because smooth muscles contain large amounts of myosin (about 10% of the total protein, about 50 μM) and MLC kinase (about 0.1% of total protein) (94), MLC kinase is believed to phosphorylate MLC in smooth muscles. However, non-muscle tissue contains much smaller amounts of myosin and MLC kinase. Rho-kinase is ubiquitously expressed in various tissues (data not shown). I have speculated that Rho-kinase phosphorylates the MLC of intact myosin and activates its ATPase in a manner dependent on Rho activation in non-muscle cells.

The molecular mechanism of smooth muscle contraction induced by Rho

Ca^{2+} mobilization into the cytoplasm increases MLC phosphorylation by the activation of MLC kinase, and induces the smooth muscle contraction. However, since the cytosolic Ca^{2+} level is not always parallel with the levels of the MLC phosphorylation and contraction, an additional mechanism to regulate the Ca^{2+} sensitivity of levels of the MLC phosphorylation and contraction has been proposed (95). Agonists cause the MLC phosphorylation and contraction of permeabilized smooth muscles at fixed submaximal concentrations of Ca^{2+} in a GTP-dependent manner (96), and Rho is implicated in this GTP-enhanced Ca^{2+} sensitivity of the smooth muscle contraction (18,97). GTPγS increases the MLC phosphorylation at submaximal Ca^{2+} concentrations in permeabilized smooth muscle cells presumably by inhibiting

myosin phosphatase through Rho (98). The GTP-enhanced Ca^{2+} sensitivity is thought to account for the vasospasm and/or certain type of hypertension, but the molecular mechanism has not been clarified. The model shown above (Fig. 20) well explains this phenomenon at the molecular level. Recently, the constitutively active Rho-kinase has been shown to provoke a contraction and proportional increase in the level of MLC phosphorylation in permeabilized smooth muscle (99). Both pathways, inactivation of myosin phosphatase and phosphorylation of MLC by Rho-kinase, are necessary for an increase in the MLC phosphorylation in permeabilized vascular smooth muscle (99). More recently, it has been reported that treatment of hypertensive rat by a specific inhibitor of Rho-kinase results in a reduction of blood pressure, suggesting that Rho-Rho-kinase pathway is involved in a certain type of hypertension. (100)

Cytoskeletal reorganization by Rho-kinase downstream of Rho

To examine whether Rho-kinase regulates the actin cytoskeletons in intact cells, constitutively active Rho-kinase (CAT) was injected into Swiss 3T3 cells. CAT induces the formation of both stress fibers and focal adhesions in serum-starved cells. The actin stress fibers induced by CAT have unusual aggregation of actin filaments. Putative dominant negative forms of Rho-kinase, including CAT-KD, RB, and PH, inhibit the LPA-induced stress fiber and focal

adhesion formation. These results suggest that Rho-kinase induces stress fiber and focal adhesion formation downstream of Rho. It is most likely that activated Rho-kinase elevates the level of myosin phosphorylation and thereby enhances acto-myosin interaction, resulted in the formation of stress fibers. Although the reason why hub-like actin filaments are present in the cells injected by GST-CAT is not clear, this may have been due to high contractility of stress fibers induced by injected GST-CAT, or to loss of proper localization for CAT in the cell.

Because injection of CAT slightly increased intensity of phalloidin-staining, Rho-kinase appears to induce actin polymerization to a small extent. The cells stimulated by LPA in the presence of staurosporine showed randomly arranged actin filaments, but the cells injected with CAT in the presence of staurosporine did not form stress fibers, indicating that there are additional pathways such as PI4,5-kinase, which induce actin polymerization downstream of Rho.

The mechanism of focal adhesion formation by Rho-kinase are not known, and there may be the other substrates for Rho-kinase concerning it. Rho-kinase may mediate plural pathways from Rho and function in cooperation with other Rho-targets. The identification of physiological substrates for Rho-kinase is necessary to understand the molecular mechanism underlying the phenomena induced by Rho-kinase. Here, the MBS of myosin phosphatase and MLC are identified

as physiological substrates for Rho-kinase. Recently, it has been reported that Rho-kinase phosphorylates several proteins such as glial fibrillary acidic protein (GFAP) stoichiometrically (101). In the case of GFAP, the phosphorylation of the head domain by Rho-kinase induces the disassembly of GFAP (101). Further studies are necessary to identify another substrates for Rho-kinase and to uncover the mechanism by which Rho-kinase functions.

ACKNOWLEDGMENTS

I thank Dr. A. Iwamatsu and Dr. K. Okawa (Kirin Brewery Co. Ltd.) for peptide sequencing, Dr. T. Ono and Dr. H. Mukai (Kobe University) for analysis of PKN, Dr. A. Hall (University college of London) for providing C3, Dr. M. Ito for analysis of myosin phosphatase, K. Chihara, K. Kimura, T. Matsui, T. Yamamoto, Y. Hamajima, and N. Nakamura for construction of plasmids, nucleotide sequencing, and preparation of proteins, and A. Takemura for secretarial assistance. I am grateful to Prof. K. Kaibuchi for general guidance, encouragement, and variable suggestion throughout the whole of this work, to Dr. M. Nakafuku, Dr. S. Kuroda, and Dr. H. Qadota for valuable discussion, and to all members of laboratory for their help and valuable discussion.

REFERENCES

1. Nobes, C., and Hall, A. (1994) *Curr-Opin-Genet-Dev.* **4**, 77-81
2. Kaibuchi, K., Mizuno, T., Fujioka, H., Yamamoto, T., Kishi, K., Fukumoto, Y., Hori, Y., and Takai, Y. (1991) *Mol Cell Biol* **11**, 2873-2880
3. Mizuno, T., Kaibuchi, K., Yamamoto, T., Kawamura, M., Sakoda, T., Fujioka, H., Matsuura, Y., and Takai, Y. (1991) *Proc Natl Acad Sci USA* **88**, 6442-6446
4. Hart, M.J., Eva, A., Evans, T., Aaronson, S.A., and Cerione, R.A. (1991) *Nature* **354**, 311-314
5. Horii, Y., Beeler, J.F., Sakaguchi, K., Tachibana, M., and Miki, T. (1994) *EMBO J* **1354**, 4776-4786
6. Habets, G.G., Scholtes, E.H., Zuydgeest, D., van der Kammen, R.A., Stam, J.C., Berns, A., and Collard, J.G. (1994) *Cell* **77**, 537-549
7. Fukumoto, Y., Kaibuchi, K., Hori, Y., Fujioka, H., Araki, S., Ueda, T., Kikuchi, A., and Takai, Y. (1990) *Oncogene* **5**, 1321-1328
8. Settleman, J., Albright, C.F., Foster, L.C., and Weinberg, R.A. (1992) *Nature* **359**, 153-154
9. Lancaster, C.A., Taylor-Harris, P.M., Self, A.J., Brill, S., van Erp, H.E., and Hall, A. (1994) *J Biol Chem* **269**, 1137-1142
10. Homma, Y., and Emori, Y. (1995) *EMBO J* **14**, 286-291
11. Ridley, A.J., and Hall, A. (1992) *Cell* **70**, 389-399

12. Ridley, A.J., and Hall, A. (1994) *EMBO J* **13**, 2600-2610
13. Paterson, H.F., Self, A.J., Garrett, M.D., Just, I., Aktories, K., and Hall, A. (1990) *J Cell Biol* **111**, 1001-1007
14. Tominaga, T., Sugie, K., Hirata, M., Morii, N., Fukata, J., Uchida, A., Imura, H., and Narumiya, S. (1993) *J Cell Biol* **120**, 1529-1537
15. Takaishi, K., Sasaki, T., Kato, M., Yamochi, W., Kuroda, S., Nakamura, T., Takeichi, M., and Takai, Y. (1994) *Oncogene* **9**, 273-279
16. Kishi, K., Sasaki, T., Kuroda, S., Itoh, T., and Takai, Y. (1993) *J Cell Biol* **120**, 1187-1195
17. Mabuchi, I., Hamaguchi, Y., Fujimoto, H., Morii, N., Mishima, M., and Narumiya, S. (1993) *Zygote* **1**, 325-331
18. Hirata, K., Kikuchi, A., Sasaki, T., Kuroda, S., Kaibuchi, K., Matsuura, Y., Seki, H., Saida, K., and Takai, Y. (1992) *J Biol Chem* **267**, 8719-8722
19. Zhang, J., King, W.G., Dillon, S., Hall, A., Feig, L., and Rittenhouse, S.E. (1993) *J Biol Chem* **268**, 22251-22254
20. Kumagai, N., Morii, N., Fujisawa, K., Nemoto, Y., and Narumiya, S. (1993) *J Biol Chem* **268**, 24535-24538
21. Chong, L.D., Traynor-Kaplan, A., Bokoch, G.M., and Schwartz, M.A. (1994) *Cell* **79**, 507-513
22. Hill, C.S., Wynne, J., and Treisman, R. (1995) *Cell* **81**, 1159-1170

23. Ridley, A.J., Paterson, H.F., Johnston, C.L., Diekmann, D., and Hall, A. (1992) *Cell* **70**, 401-410

24. Nishiyama, T., Sasaki, T., Takaishi, K., Kato, M., Yaku, H., Araki, K., Matsuura, Y., and Takai, Y. (1994) *Mol Cell Biol* **14**, 2447-2456

25. Johnson, D.I., and Pringle, J.R. (1990) *J Cell Biol* **111**, 143-152

26. Nobes, C.D., and Hall, A. (1995) *Cell* **81**, 53-62

27. Kozma, R., Ahmed, S., Best, A., and Lim, L. (1995) *Mol Cell Biol* **15**, 1942-1952

28. Manser, E., Leung, T., Salihuddin, H., Zhao, Z.S., and Lim, L. (1994) *Nature* **367**, 40-46

29. Martin, G.A., Bollag, G., McCormick, F., and Abo, A. (1995) *EMBO J* **14**, 1970-1978

30. Aspenstrom, P., Lindberg, U., and Hall, A. (1996) *Curr Biol* **6**, 70-75

31. Symons, M., Derry, J.M., Karlak, B., Jiang, S., Lemahieu, V., Mccormick, F., Francke, U., and Abo, A. (1996) *Cell* **84**, 723-734

32. Hart, M.J., Callow, M.G., Souza, B., and Polakis, P. (1996) *EMBO J* **15**, 2997-3005

33. Brill, S., Li, S., Lyman, C.W., Church, D.M., Wasmuth, J.J., Weissbach, L., Bernards, A., and Snijders, A.J. (1996) *Mol Cell Biol* **16**, 4869-4878

34. McCallum, S.J., Wu, W.J., and Cerione, R.A. (1996) *J Biol Chem* **271**, 21732-21737

35. Kuroda, K., Fukara, M., Kobayashi, K., Nakafuku, M., Nomura, N., Iwamatsu, A., and Kaibuchi, K. (1996) *J Biol Chem* **271**, 23363-23367

36. Van Aelst, L., Joneson, T., and Bar-Sagi, D. (1996) *EMBO J* **15**, 3778-3786

37. Zheng, Y., Bagrodia, S., and Cerione, R.A. (1994) *J Biol Chem* **2692**, 18727-18730

38. Amano, M., Mukai, H., Ono, Y., Chihara, K., Matsui, T., Hamajima, Y., Okawa, K., Iwamatsu, A., and Kaibuchi, K. (1996) *Science* **271**, 648-650

39. Matsui, T., Amano, M., Yamamoto, T., Chihara, K., Nakafuku, M., Ito, M., Nakano, T., Okawa, K., Iwamatsu, A., and Kaibuchi, K. (1996) *EMBO J.* **15**, 2208-2216

40. Kimura, K., Ito, M., Amano, M., Chihara, K., Fukata, Y., Nakafuku, M., Yamamori, B., Feng, J., Nakano, T., Okawa, K., Iwamatsu, A., and Kaibuchi, K. (1996) *Science* **273**, 245-248

41. Amano, M., Ito, M., Kimura, K., Fukata, Y., Chihara, K., Nakano, T., Matsuura, Y., and Kaibuchi, K. (1996) *J Biol Chem* **271**, 20246-20249

42. Amano, M., Chihara, K., Kimura, K., Fukata, Y., Nakamura, N., Matsuura, Y., and Kaibucni, K. (1997) *Science* **275**, 1308-1311

43. Bar-Sagi, D. (1995) *Methods Enzymol* **255**, 436-442

44. Spudich, J.A., and Watt, S. (1971) *J Biol Chem* **246**, 4866-4871

45. Mizushima, S., and Nagata, S. (1990) *Nucleic Acids Res* **18**, 5322

46. Kikuchi, A., Yamashita, T., Kawata, M., Yamamoto, K., Ikeda, K., Tanimoto, T., and Takai, Y. (1988) *J Biol Chem* **263**, 2897-2904

47. Sambrook, J., Fritsch, E.F., and Maniatis, T., (Cold Spring Harbor Laboratory Press, Cold Spring Harbor, NY, 1989)

48. Alting-Mees, M.A., and Short, J.M. (1989) *Nucleic Acids Res* **17**, 9494

49. Manser, E., Leung, T., Monfries, C., Teo, M., Hall, C., and Lim, L. (1992) *J Biol Chem* **267**, 16025-16028

50. Chen, Y.H., Chen, M.X., Alessi, D.R., Campbell, D.G., Shanahan, C., Cohen, P., and Cohen, P.T. (1994) *Febs Lett* **356**, 51-55

51. Taylor, D.A., and Stull, J.T. (1988) *J Biol Chem* **263**, 14456-14462

52. Ikebe, M., Barsotti, R.J., Hinkins, S., and Hartshorne, D.J. (1984) *Biochemistry* **23**, 5062-5068

53. Laemmli, U.K. (1970) *Nature* **227**, 680-685

54. Naka, M., Nishikawa, M., Adelstein, R.S., and Hidaka, H. (1983) *Nature* **306**, 490-492

55. Hunter, T., and Sefton, B.M. (1980) *Proc Natl Acad Sci USA* **77**, 1311-1315

56. Harlow, E., and Lame, D., (Cold Spring Habor laboratory, Cold Spring Harbor, NY, 1988)

57. Mukai, H., and Ono, Y. (1994) *Biochem Biophys Res Commun* **199**, 897-904

58. Palmer, R.H., Ridden, J., and Parker, P.J. (1995) *Eur J Biochem* **227**, 344-351

59. Shimizu, H., Ito, M., Miyahara, M., Ichikawa, K., Okubo, S., Konishi, T., Naka, M., Tanaka, T., Hirano, K., Hartshorne, D.J., and Nakano, T. (1994) *J Biol Chem* **269**, 30407-30411

60. Kozak, M. (1987) *Nucleic Acids Res* **15**, 8125-8148

61. Brook, J.D., McCurrach, M.E., Harley, H.G., Buckler, A.J., Church, D., Aburatani, H., Hunter, K., Stanton, V.P., Thirion, J.P., Hudson, T., Sohn, R., Zemelman, B., Snell, R.G., Rundle, S.A., Crow, S., Davies, J., Shelbourne, P., Buxton, J., Jones, C., Juvonen, V., Johnson, K., Harper, P.S., Shaw, D.J., and Housman, D.E. (1992) *Cell* **68**, 799-808

62. Fu, Y.H., Pizzuti, A., Fenwick, R.G., Jr., King, J., Rajnarayan, S., Dunne, P.W., Dubel, J., Nasser, G.A., Ashizawa, T., de Jong, P., Wieringa, B., Korneluk, R., Perryman, B., Epstein, H.F., and Caskey, C.T. (1992) *Science* **255**, 1256-1258

63. Mahadevan, M., Tsilfidis, C., Sabourin, L., Shutler, G., Amemiya, C., Jansen, G., Neville, C., Narang, M., Barcelo, J., O'Hoy, K., Leblond, S., Earle-Macdonald, J., De Jong, P.J., Wieringa, B., and R.G., K. (1992) *Science* **255**, 1253-1255

64. Takai, Y., Sasaki, T., Tanaka, K., and Nakanishi, H. (1995) *Trends Biochem Sci* **20**, 227-231

65. Clark, E.A., and Brugge, J.S. (1995) *Science* **268**, 233-239

66. Aizawa, H., Emori, Y., Murofushi, H., Kawasaki, H., Sakai, H., and Suzuki, K. (1990) *J Biol Chem* **265**, 13849-13855

67. Trinkle-Mulcahy, L., Ichikawa, K., Hartshorne, D.J., Siegman, M.J., and Butler, T.M. (1995) *J Biol Chem* **270**, 18191-18194

68. Tan, J.L., Ravid, S., and Spudich, J.A. (1992) *Annu Rev Biochem* **61**, 721-759

69. Ikebe, M., and Hartshorne, D.J. (1985) *J Biol Chem* **260**, 10027-10031

70. Kamisoyama, H., Araki, Y., and Ikebe, M. (1994) *Biochemistry* **33**, 840-847

71. Bresnick, A.R., Wolff-Long, V.L., Baumann, O., and Pollard, T.D. (1995) *Biochemistry* **34**, 12576-12583

72. Nishikawa, M., Sellers, J.R., Adelstein, R.S., and Hidaka, H. (1984) *J Biol Chem* **259**, 8808-8814

73. Bengur, A.R., Robinson, E.A., Appella, E., and Sellers, J.R. (1987) *J Biol Chem* **262**, 7613-7617

74. Ikebe, M., and Reardon, S. (1990) *Biochemistry* **29**, 2713-2720

75. Nishizuka, Y. (1988) *Nature* **334**, 661-665

76. Hanks, S.K., Quinn, A.M., and Hunter, T. (1988) *Science*

241, 42-52

77. Rapp, U.R. (1991) *Oncogene* **6**, 495-500

78. Kaibuchi, K., Fukumoto, Y., Oku, N., Takai, Y., Arai, K., and Muramatsu, M. (1989) *J Biol Chem* **264**, 13489-13496

79. Hirai, S., Izumi, Y., Higa, K., Kaibuchi, K., Mizuno, K., Osada, S., Suzuki, K., and Ohno, S. (1994) *EMBO J* **13**, 2331-2340

80. Ridley, A.J., Comoglio, P.M., and Hall, A. (1995) *Mol Cell Biol* **15**, 1110-1122

81. Aktories, K., Braun, U., Rosener, S., Just, I., and Hall, A. (1989) *Biochem Biophys Res Commun* **158**, 209-213

82. Sekine, A., Fujiwara, M., and Narumiya, S. (1989) *J Biol Chem* **264**, 8602-8605

83. Alessi, D., MacDougall, L.K., Sola, M.M., Ikebe, M., and Cohen, P. (1992) *Eur J Biochem* **210**, 1023-1035

84. Okubo, S., Erdodi, F., Ito, M., Ichikawa, K., Konishi, T., Nakano, T., Kawamura, T., Brautigan, D.L., and Hartoshorne, D.J. (1993) *Adv Prot Phosphatase* **7**, 295-314

85. Harper, P.S., (W. B. Saunders Co., London, 1989)

86. Watanabe, G., Saito, Y., Madaule, P., Ishizaki, T., Fujisawa, K., Morii, N., Mukai, H., Ono, Y., Kakizuka, A., and Narumiya, S. (1996) *Science* **271**, 645-648

87. Leung, T., Manser, E., Tan, L., and Lim, L. (1995) *J Biol Chem* **270**, 29051-29054

88. Ishizaki, T., Maekawa, M., Fujisawa, K., Okawa, K., Iwamatsu, A., Fujita, A., Watanabe, N., Saito, Y., Kakizuka, A., Morii, N., and Narumiya, S. (1996) *EMBO J* **15**, 1885-1893

89. Madaule, P., Furuyashiki, T., Reid, T., Ishizaki, T., Watanabe, G., Morii, N., and Narumiya, S. (1995) *Febs Lett* **377**, 243-248

90. Watanabe, N., Madaule, P., Reid, T., Ishizaki, T., Watanabe, G., Kakizuka, A., Saito, Y., Nakao, K., Jockusch, B.M., and Narumiya, S. (1997) *EMBO J* **16**, 3044-3056

91. Hartshorne, D.J. (1987), in *Physiology of the Gastrointestinal tract* (Johnson, D.R., eds) pp. 423-482, Raven Press, New York

92. Sellers, J.R., and Adelstein, R.S. (1987), in *The Enzymes* (Boyer, P., and Erevs, E.G., eds) Vol.18 pp. 381-418, Academic Press, San Diego

93. Kamm, K.E., Hsu, L.C., Kubota, Y., and Stull, J.T. (1989) *J Biol Chem* **264**, 21223-21229

94. Kamm, K.E., and Stull, J.T. (1985) *Annu Rev Pharmacol Toxicol* **25**, 593-603

95. Bradley, A.B., and Morgan, K.G. (1987) *J Physiol* **385**, 437-448

96. Kitazawa, T., Masuo, M., and Somlyo, A.P. (1991) *Proc Natl Acad Sci USA* **88**, 9307-9310

97. Gong, M.C., Iizuka, K., Nixon, G., Browne, J.P., Hall,

A., Eccleston, J.F., Sugai, M., Kobayashi, S., Somlyo, A.V., and Somlyo, A.P. (1996) *Proc Natl Acad Sci USA.* **93**, 1340-1345

98. Noda, M., Yasuda-Fukazawa, C., Moriishi, K., Kato, T., Okuda, T., Kurokawa, K., and Takuwa, Y. (1995) *Febs Lett* **367**, 246-250

99. Kureishi, Y., Kobayashi, S., Amano, M., Kimura, K., Kanaide, H., Nakano, T., Kaibuchi, K., and Ito, M. (1997) *J Biol Chem* **272**, 12257-12260

100. Uehata, M., Ishizaki, T., Satoh, H., Ono, T., Kawahara, T., Morishita, T., Tamakawa, H., Yamagami, K., Inui, J., Maekawa, M., and Narumiya, S. (1997) *Nature* **389**, 990-994

101. Kosako, H., Amano, M., Yanagida, M., Tanabe, K., Nishi, Y., Kaibuchi, K., and Inagaki, M. (1997) *J Biol Chem* **272**, 10333-10336

Abbreviations

The Abbreviations used are: GAP, GTPase-activating proteins; LPA, lysophosphatidic acid; PI3-kinase, phosphatidylinositol 3-kinase; PI4,5-kinase, phosphatidylinositol 4-phosphate 5-kinase; PKN, protein kinase N; MBS, myosin-binding subunit; MLC, myosin light chain; GST, glutathione *S*-transferase; C3, C3 transferase; MBP, maltose binding protein; Sf9, *Spodoptera frugiperda*; DTT, dithiothreitol; GTPγS, guanosine 5'-(3-*O*-thio)triphosphate; BSA, bovine serum albumin; PBS, phosphate buffered saline; CHAPS, 3-[(3-Cholamidopropyl) dimethylammonio] propanesulfonic acid; IPTG, isopropyl-β-D-thiogalactopyranoside; TCA, trichloroacetic acid; DMEM, Dulbecco's modified Eagle's medium; TRITC, tetramethyl rhodamine B isothiocyanate; PH, pleckstrin-homology; PKC, protein kinase C.

FIGURE LEGENDS

Fig. 1. Purification of RhoA-interacting proteins by GST-RhoA affinity column chromatography. The crude membrane extract was loaded on a glutathione-Sepharose column containing either GST, GDP·GST-RhoA, GTPγS·GST-RhoA, GTPγS·GST-RhoA^{A37}, GDP·GST-Rac1, or GTPγS·GST-Rac1. Bound proteins were eluted with the respective GST-fusion proteins by the addition of glutathione. Portions (45 μl each) from the glutathione-eluted fractions were subjected to SDS-PAGE followed by silver staining. GST (lane 1), GDP·GST-RhoA (lane 2), GTPγS·GST-RhoA (lane 3), GTPγS·GST-RhoA^{A37} (lane 4), GDP·GST-Rac1 (lane 5), GTPγS·GST-Rac1 (lane 6).

Fig. 2. Deduced amino acid sequence of p164 (Rho-kinase). Amino acid sequences determined from native p164 (Rho-kinase) are indicated by single underlines. Amino acid sequences used for oligonucleotide probes are indicated by double underlines. The GenBank accession number is U36909.

Fig. 3. Schematic representation of Rho-kinase and myotonic dystrophy kinase. The numbers indicate the amino acid sequence homology in the kinase domain.

Fig. 4. Complex formation between recombinant PKN and GTPγS·GST-RhoA in a cell-free system. MBP-PKN-N was mixed with glutathione-Sepharose beads coated with either GST, GDP·GST-RhoA, GTPγS·GST-RhoA, GTPγS·GST-RhoA^{A37}, GDP·GST-Rac1, GTPγS·GST-Rac1, GDP·GST-H-Ras, or GTPγS·GST-H-Ras, and MBP-PKN-N was eluted by the addition of

glutathione. GST (lane 1), GDP·GST-RhoA (lane 2), GTPγS·GST-RhoA (lane 3), GTPγS·GST-RhoA^{A37} (lane 4), GDP·GST-Rac1 (lane 5), GTPγS·GST-Rac1 (lane 6), GDP·GST-H-Ras (lane 7), GTPγS·GST-H-Ras (lane 8).

Fig. 5. Direct binding of activated RhoA to Rho-kinase. Nitrocellulose filters containing the membrane extract (lanes 1 and 3) and purified Rho-kinase (lanes 2 and 4) separated by SDS-PAGE were probed with [^{35}S]GTPγS·GST-RhoA (lanes 1 and 2) or [^{35}S]GTPγS·GST-RhoA^{A37} (lanes 3 and 4). The arrow denotes the position of Rho-kinase. The results shown are representative of three independent experiments.

Fig. 6. Effects of various small GTPases on the kinase activity of PKN. The kinase reaction was done with PKCα peptide (40 μM) in the presence of various small GTPases (50 pmol each) as indicated. The values shown are means ± S.E. of triplicates. Since purified PKN is labile, I used it for the kinase assay in a day after purification.

Fig. 7. Phosphorylation of MBS by Rho-kinase. The kinase reaction was carried out with C-terminus of rat MBS-C (699-976 amino acids) as a fusion protein with MBP (50 nM) in the presence of either GST (lane 1), GDP·GST-RhoA (lane 2), or GTPγS·GST-RhoA (lane 3) (1 μM each). The arrow denotes the position of MBS. The results shown are representative of three independent experiments.

Fig. 8. Phosphorylation of MBS and inhibition of the MLC phosphatase activity by Rho-kinase. MBS of native myosin phosphatase was thiophosphorylated in the presence of the indicated amounts of Rho-kinase with or without GTPγS·GST-RhoA. Under the similar conditions, the MLC phosphatase activity was measured after MBS was thiophosphorylated. Ten μl of the sample was subjected to the MLC phosphatase assay. (○),(●), thiophosphorylation of MBS; (□),(■), MLC phosphatase activity in the presence of ATPγS; (◊), MLC phosphatase activity in the absence of ATPγS. (●),(■), with GTPγS·GST-RhoA; (○),(□), without GTPγS·GST-RhoA. The values shown are means ± S.E. of triplicates.

Fig. 9. Phosphorylation of MBS in NIH 3T3 cell lines. Upper panel; Phosphorylation of MBS in NIH 3T3 cell and the cells expressed RhoA (RhoA-5, RhoA-24) or $RhoA^{V14}$ ($RhoA^{V14}$-7, $RhoA^{V14}$-25) was measured. The values in parentheses show stimulation fold of MBS phosphorylation. The results are shown from an autoradiograph. Lower panel; Expression level of MBS in NIH 3T3 cell and the cells expressed RhoA (RhoA-5, RhoA-24) or $RhoA^{V14}$ ($RhoA^{V14}$-7, $RhoA^{V14}$-25) was indicated. The results are representative of three independent experiments.

Fig. 10. Phosphorylation of MLC in NIH 3T3 cell lines. Extent of MLC phosphorylation in NIH 3T3 cells and the cells overexpressing RhoA or $RhoA^{V14}$ was determined. CLA, calyculin-A; MLCP and $MLCP_2$, monophosphorylated and

diphosphorylated MLC. The values show the percentage of MLCP and $MLCP_2$ in total MLC. The values shown are means ± S.E. of triplicates. The values for total MLC phosphorylation were compared by Dunnett's t test. ($^{*}p<0.01$, $^{**}P<0.001$)

Fig. 11. Phosphorylation of MLC by Rho-kinase. Isolated MLC (0.5 μg of protein) was phosphorylated by Rho-kinase in the presence of either GST (lane 1), GDP·GST-RhoA (lane 2), GTPγS·GST-RhoA (lane 3), GTPγS·GST-$RhoA^{A37}$ (lane 4), GDP·GST-Rac1 (lane 5) or GTPγS·GST-Rac1 (lane 6), GST-CAT (lane 7), or by MLC kinase in the absence (lane 8) or presence (lane 9) of Ca^{2+} and calmodulin. Intact myosin (5 μg of protein) was phosphorylated by Rho-kinase in the absence (lane 10) or presence (lane 11) of GTPγS·GST-RhoA. The phosphorylated MLC was resolved by a SDS-PAGE and visualized by an image analyzer. The results are representative of three independent experiments.

Fig. 12. Phosphorylation of MLC by Rho-kinase. Various doses of MLC were phosphorylated by Rho-kinase (25 ng of protein) in the absence (○) or presence (●) of GTPγS·GST-RhoA , by GST-CAT (7.5 ng of protein) (▲) or by MLC kinase (7.5 ng of protein) in the absence (□) or presence (■) of Ca^{2+} and calmodulin. The values shown are means ± S.E. of triplicates.

Fig. 13. A phosphopeptide map analysis of MLC. MLC (0.5 μg of protein) was phosphorylated by Rho-kinase, MLC

kinase or PKC. Phosphorylated MLC was digested with trypsin and each sample was loaded onto a silica gel plate. Phosphopeptides were separated by electrophoresis (horizontal dimension) and chromatography (vertical dimension), and then were visualized by an image analyzer. Asterisks denote origins.

Fig. 14. Effect of phosphorylation of myosin by Rho-kinase on the MgATPase activity that was activated by actin. Myosin was incubated with GST-CAT (■) or with MLC kinase (◆), or without kinase (●). After incubation, the ATPase activity was measured at the various concentrations of F-actin. The values shown are means ± S.E. of triplicates.

Fig. 15. Dominant active form of Rho-kinase. MLC was phosphorylated by Rho-kinase or GST-CAT in the presence or absence of GTPγS·GST-RhoA (1.5 μM). Data are means ± SEM of triplicate determinations.

Fig. 16. Effects of dominant negative form of Rho-kinase or staurosporine on Rho-kinase. MLC was phosphorylated by Rho-kinase in the presence of GTPγS·GST-RhoA or by GST-CAT with GST-RB or staurosporine. Data are means ± SEM of triplicate determinations.

Fig. 17. Actin reorganization caused by Rho-kinase. Actin filaments in confluent, serum-starved Swiss 3T3 cells stimulated with vehicle (a), with LPA (200 ng/ml) for 15 min without injection (b), microinjected with C3 (80 μg/ml) and

stimulated by LPA (c), stimulated by LPA 15 min after treatment with 100 nM staurosporine (d), microinjected with GST-CAT (0.5 mg/ml) alone (e), microinjected with GST-CAT and C3 (f), and microinjected with GST-CAT 15 min after treatment with staurosporine (g).

Fig. 18. Focal adhesion formation induced by Rho-kinase. Vinculin localization is shown. Symbols are the same as those in Fig. 17 except that actin filaments and vinculin localization are shown in Swiss 3T3 cells microinjected with GST-CAT (h). The arrow heads show the injected cells. Bar represents 20 μm.

Fig. 19. Effect of various forms of Rho-kinase on LPA-induced actin filament reorganization and focal adhesion formation. Confluent, serum-starved Swiss 3T3 cells were microinjected with GST-CAT-KD (2 mg/ml) (A,E), with GST-COIL (5 mg/ml) (B,F), with GST-RB (5 mg/ml) (C,G) or with GST-PH (5 mg/ml) (D,H), and then stimulated with LPA (200 ng/ml). Actin filaments and vinculin localization are shown. The arrow heads show the injected cells. Bar represents 20 μm.

Fig. 20. Model for the regulation of MLC phosphorylation by Rho, Rho-kinase and myosin phosphatase. Cat, catalytic subunit of myosin phosphatase.

Fig. 1

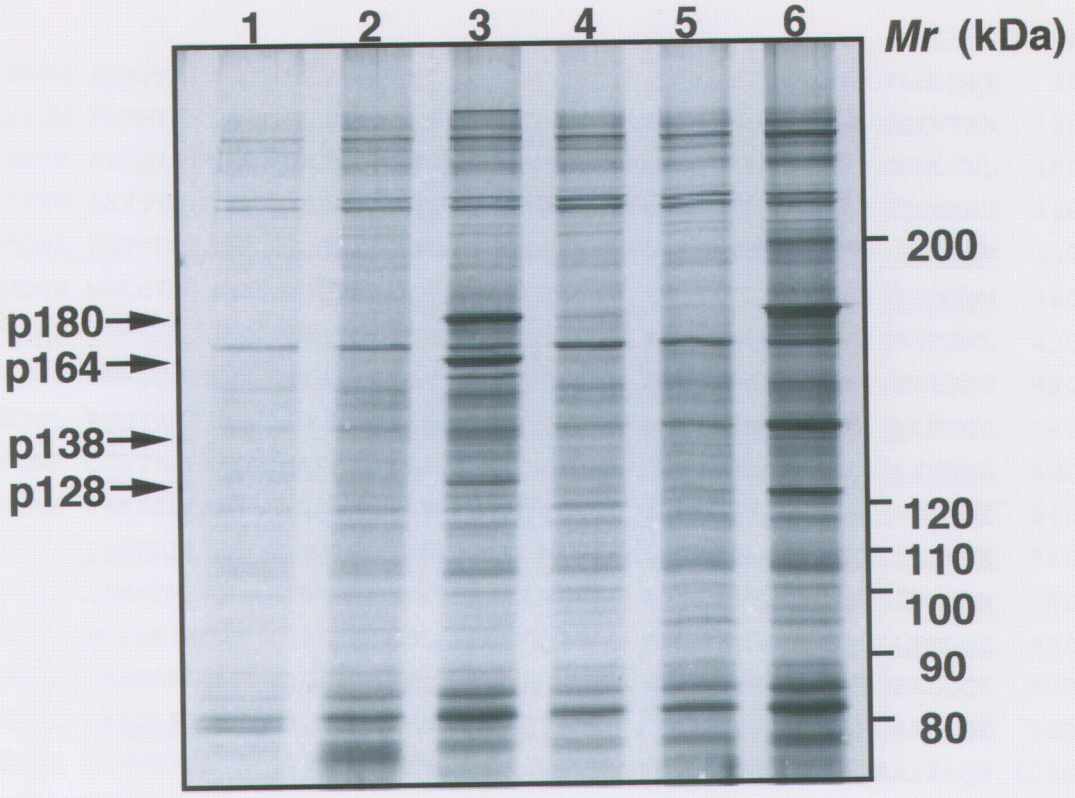

Fig. 2

```
MSRPPPTGKM PGAPEAVSGD GAGASRQRKL EALIRDPRSP INVESLLDGL NPLVLDLDFP   60
ALRKNKNIDN FLNRYEKIVK KIRGLQMKAE DYDVVKVIGR GAFGEVQLVR HKASQKVYAM  120
KLLSKFEMIK RSDSAFFWEE RDIMAFANSP WVVQLFCAFQ DDKYLYMVME YMPGGDLVNL  180
MSNYDVPEKW AKFYTAEVVL ALDAIHSMGL IHRDVKPDNM LLDKHGHLKL ADFGTCMKMD  240
ETGMVHCDTA VGTPDYISPE VLKSQGGDGY YGRECDWWSV GVFLFEMLVG DTPFYADSLV  300
GTYSKIMDHK NSLCFPEDAE ISKHAKNLIC AFLTDREVRL GRNGVEEIKQ HPFFKNDQWN  360
WDNIRETAAP VVPELSSDID SSNFDDIEDD KGDVETFPIP KAFVGNQLPF IGFTYYRENL  420
LLSDSPSCKE NDSIQSRKNE ESQEIQKKLY TLEEHLSTEI QAKEELEQKC KSVNTRLEKV  480
AKELEEEITL RKNVESTLRQ LEREKALLQH KNAEYQRKAD HEADKKRNLE NDVNSLKDQL  540
EDLKKRNQNS QISTEKVNQL QRQLDETNAL LRTESDTAAR LRKTQAESSK QIQQLESNNR  600
DLQDKNCLLE TAKLKLEKEF INLQSVLESE RRDRTHGSEI INDLQGRISG LEEDVKNGKI  660
LLAKVELEKR QLQERFTDLE KEKNNMEIDM TYQLKVIQQS LEQEETEHKA TKARLADKNK  720
IYESIEEAKS EAMKEMEKKL SEERTLKQKV ENLLLEAEKR CSILDCDLKQ SQQKINELLK  780
QKDVLNEDVR NLTLKIEQET QKRCLTQNDL KMQTQQVNTL KMSEKQLKQE NNHLLEMKMS  840
LEKQNAELRK ERQDADGQMK ELQDQLEAEQ YFSTLYKTQV RELKEECEEK TKLCKELQQK  900
KQELQDERDS LAAQLEITLT KADSEQLARS IAEEQYSDLE KEKIMKELEI KEMMARHKQE  960
LTEKDATIAS LEETNRTLTS DVANLANEKE ELNNKLKEAQ EQLSRLKDEE ISAAAIKAQF 1020
EKQLLTERTL KTQAVNKLAE IMNRKEPVKR GNDTDVRRKE KENRKLHMEL KSEREKLTQQ 1080
MIKYQKELNE MQAQIAEESQ IRIELQMTLD SKDSDIEQLR SQLQALHIGL DSSSIGSGPG 1140
DTEADDGFPE SRLEGWLSLP VRNNTKKFGW VKKYVIVSSK KILFYDSEQD KEQSNPYMVL 1200
DIDKLFHVRP VTQTDVYRAD AKEIPRIFQI LYANEGESKK EQEFPVEPVG EKSNYICHKG 1260
HEFIPTLYHF PTNCEACMKP LWHMFKPPPA LECRRCHIKC HKDHMDKKEE IIAPCKVYYD 1320
ISSAKNLLLL ANSTEEQQKW VSRLVKKIPK KPPAPDPFAR SSPRTSMKIQ QNQSIRRPSR 1380
QLAPNKPS                                                          1388
```

Fig. 3

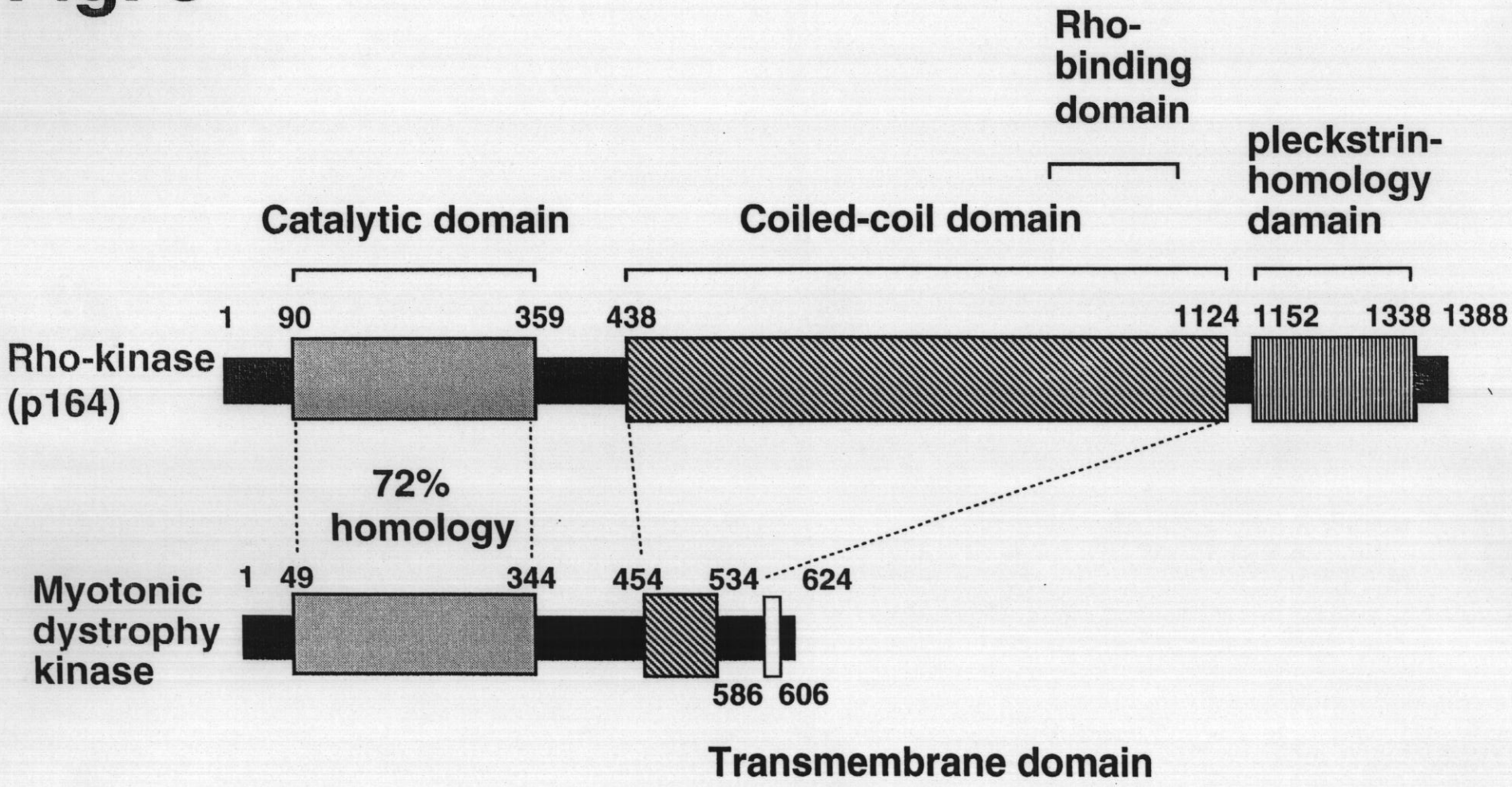
Rho-
binding
domain
pleckstrin-
homology
damain
Catalytic domain
Coiled-coil domain
1
90
359
438
1124
1152
1338
1388
Rho-kinase
(p164)
72%
homology
1
49
344
454
534
624
Myotonic
dystrophy
kinase
586
606
Transmembrane domain

Fig. 4

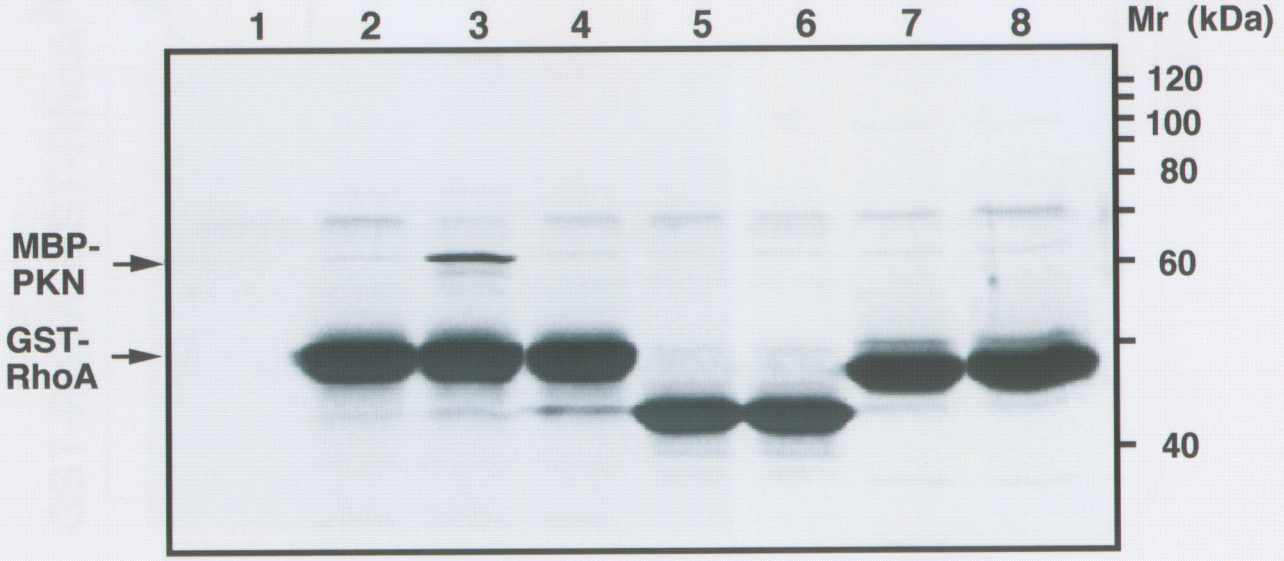

Fig. 5

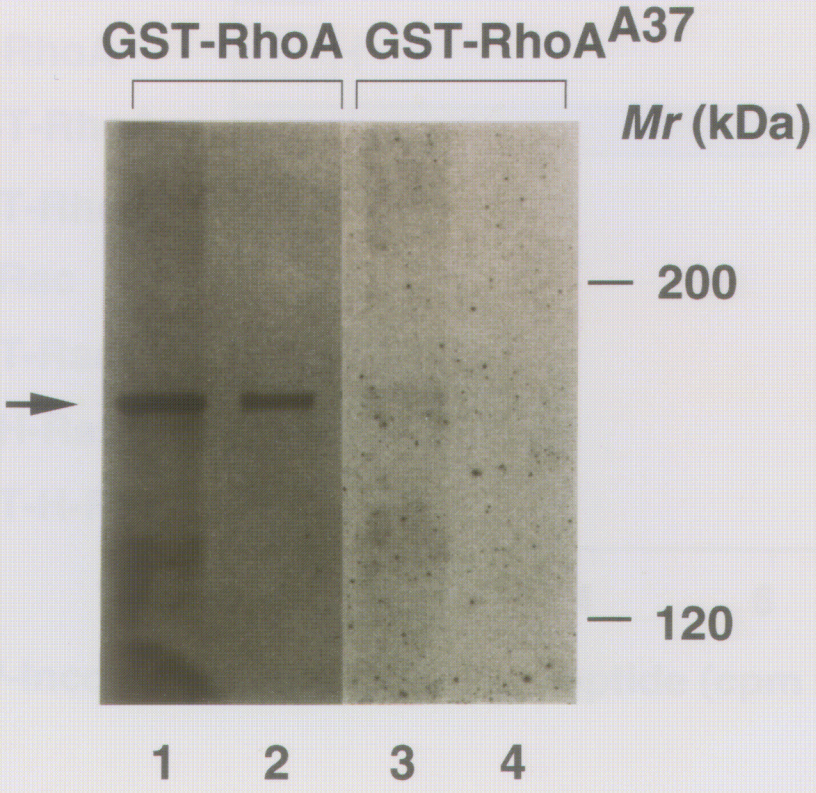

Fig. 6

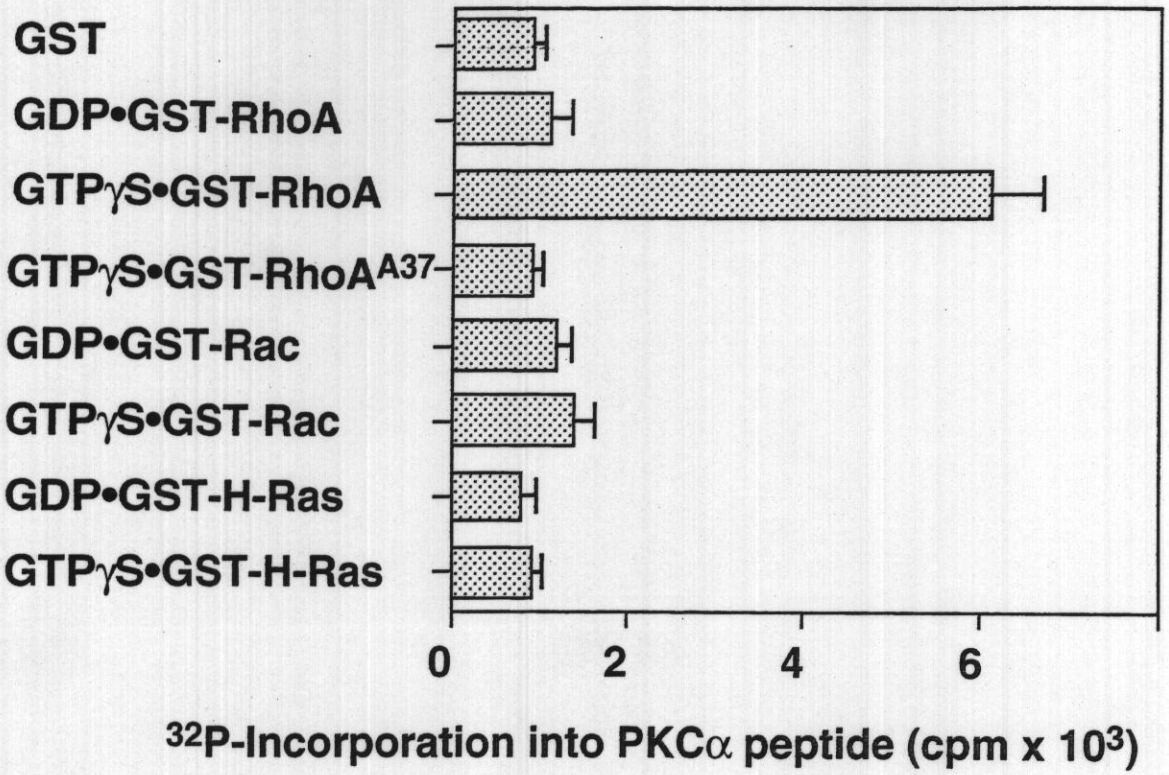
GST
GDP•GST-RhoA
GTPγS•GST-RhoA
GTPγS•GST-RhoA^{A37}
GDP•GST-Rac
GTPγS•GST-Rac
GDP•GST-H-Ras
GTPγS•GST-H-Ras
0
2
4
6
^{32}P-Incorporation into PKCα peptide (cpm x 10^3)

Fig. 7

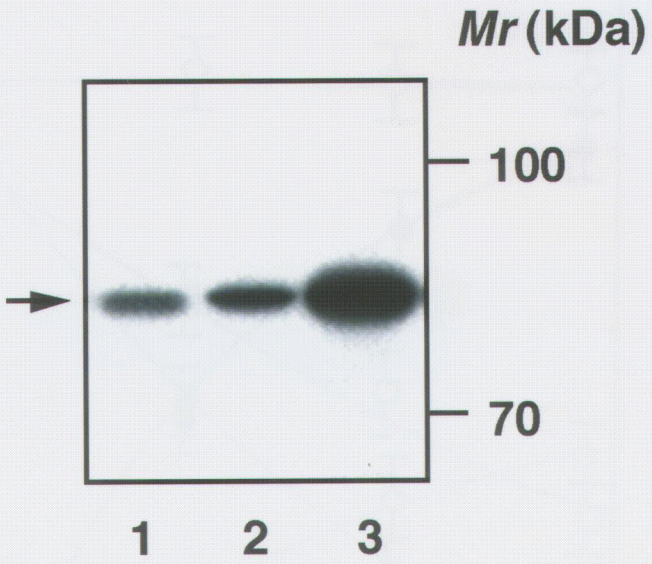

Fig. 8

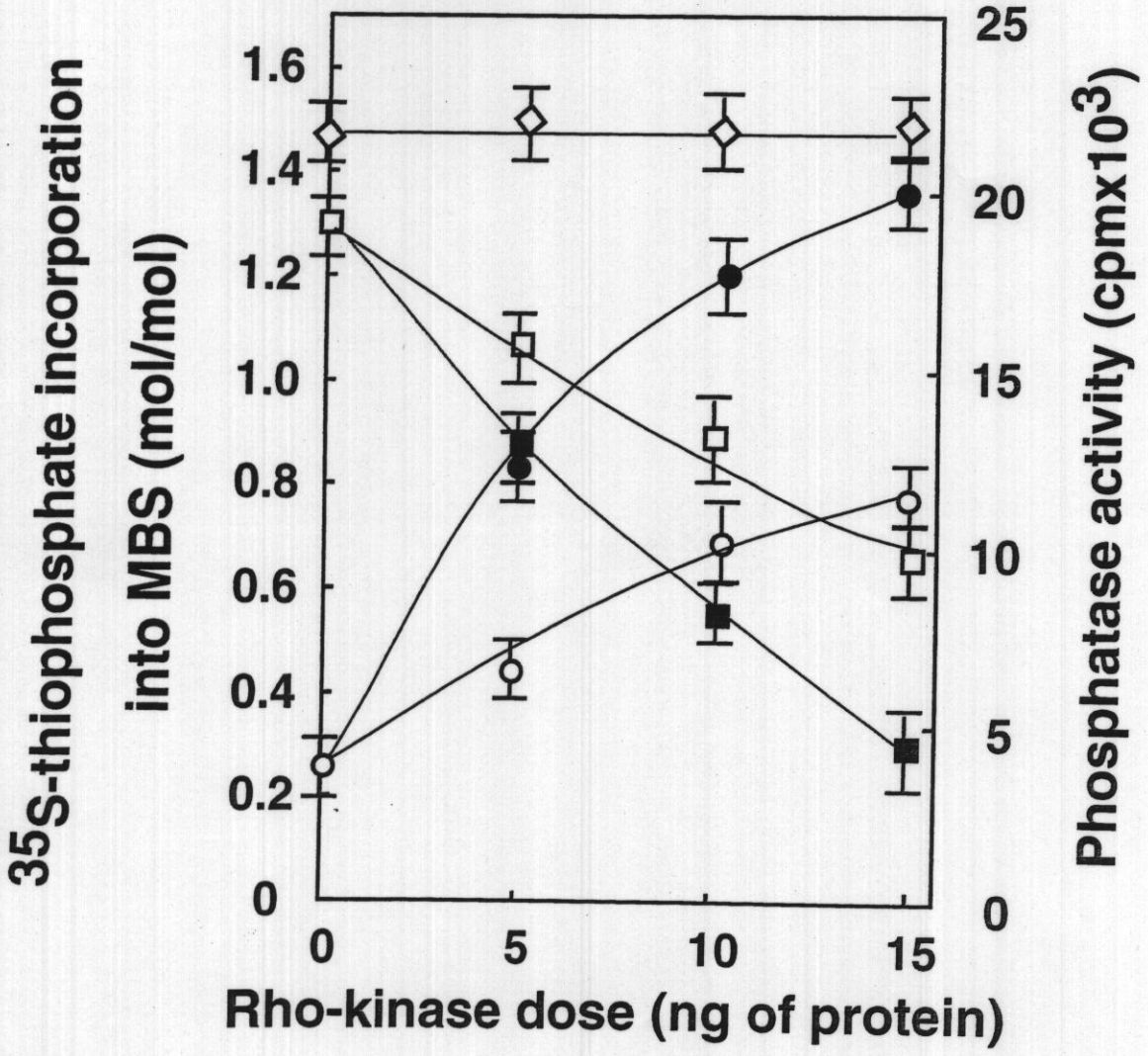
35S-thiophosphate incorporation into MBS (mol/mol)
Phosphatase activity (cpmx10^3)
Rho-kinase dose (ng of protein)
0
0.2
0.4
0.6
0.8
1.0
1.2
1.4
1.6
0
5
10
15
20
25
0
5
10
15

Fig. 9

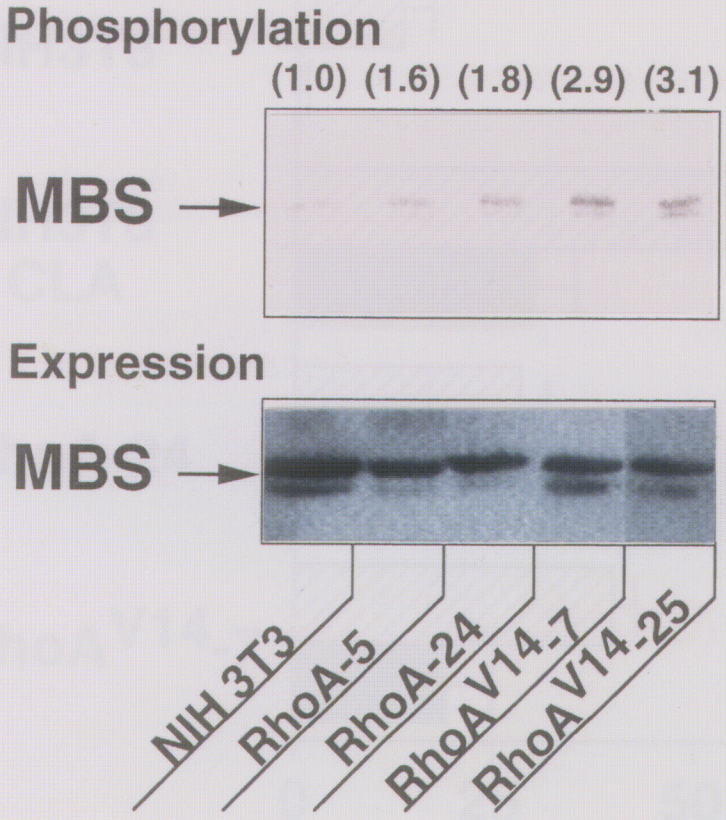
Phosphorylation
(1.0) (1.6) (1.8) (2.9) (3.1)
MBS
Expression
MBS
NIH 3T3
RhoA-5
RhoA-24
RhoA V14-7
RhoA V14-25

Fig.10

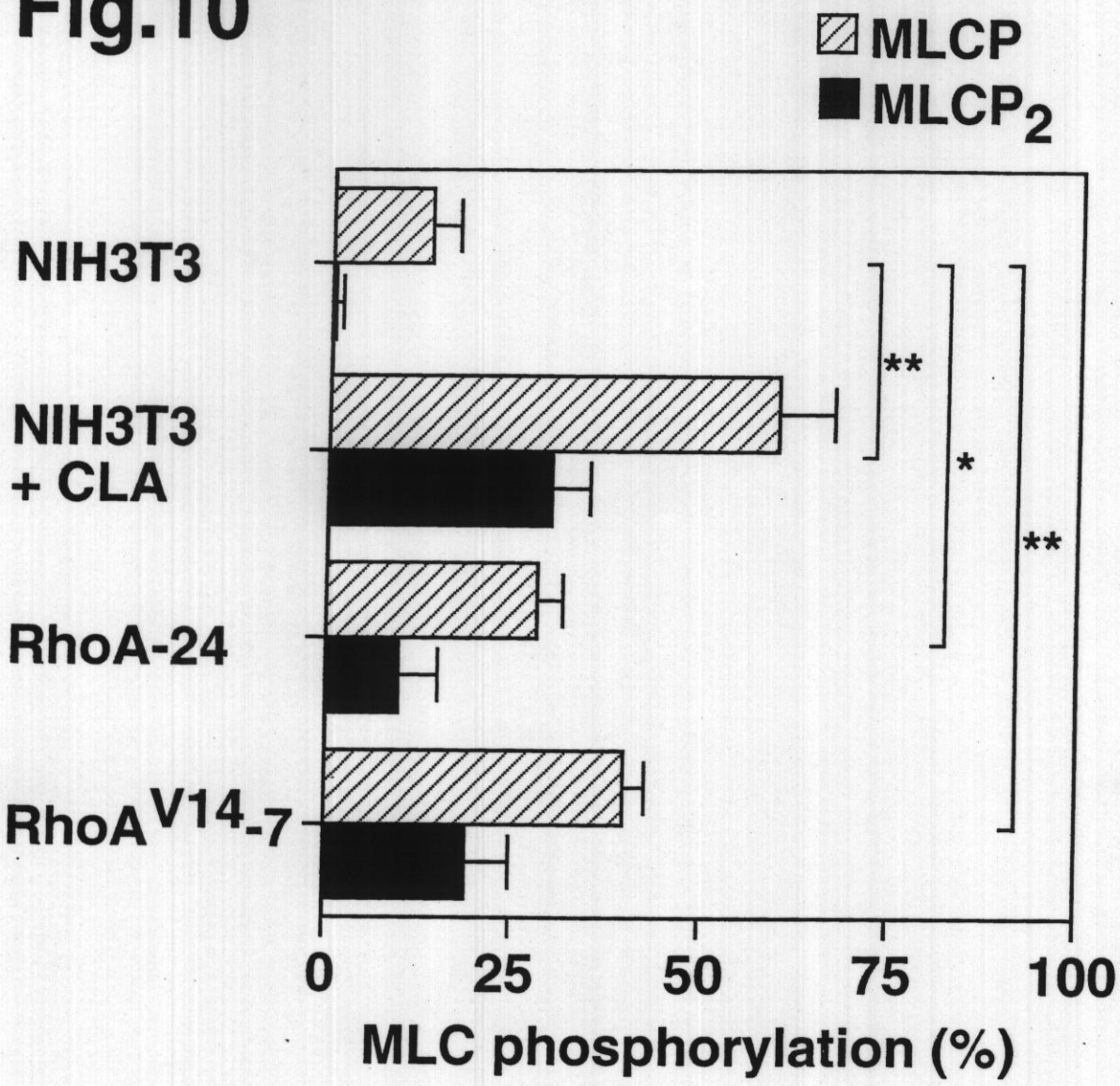
MLCP
MLCP2
NIH3T3
NIH3T3
+ CLA
RhoA-24
RhoAV14-7
**
*
**
0
25
50
75
100
MLC phosphorylation (%)

Fig. 11

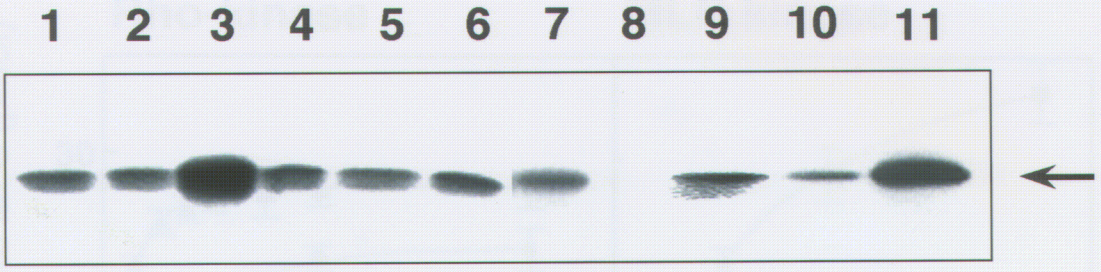

Fig. 12

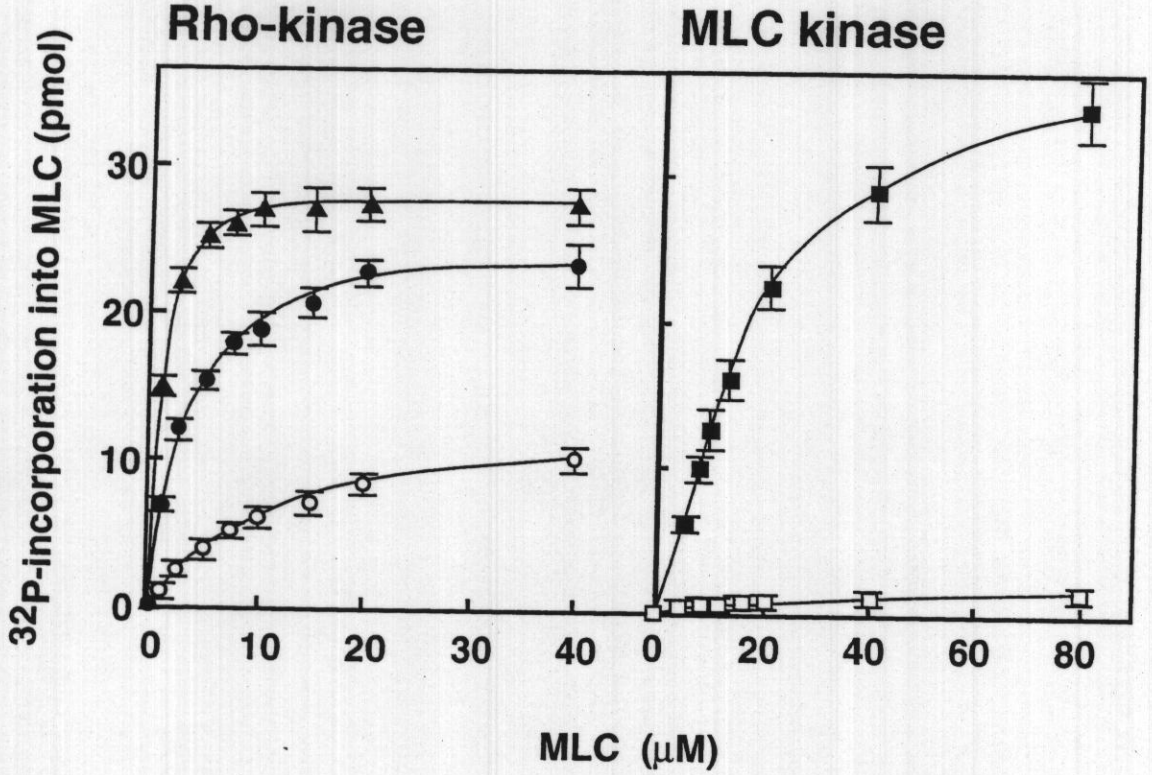
Rho-kinase
MLC kinase
^{32}P-incorporation into MLC (pmol)
0
10
20
30
0
10
20
30
40
0
20
40
60
80
MLC (μM)

Fig. 13

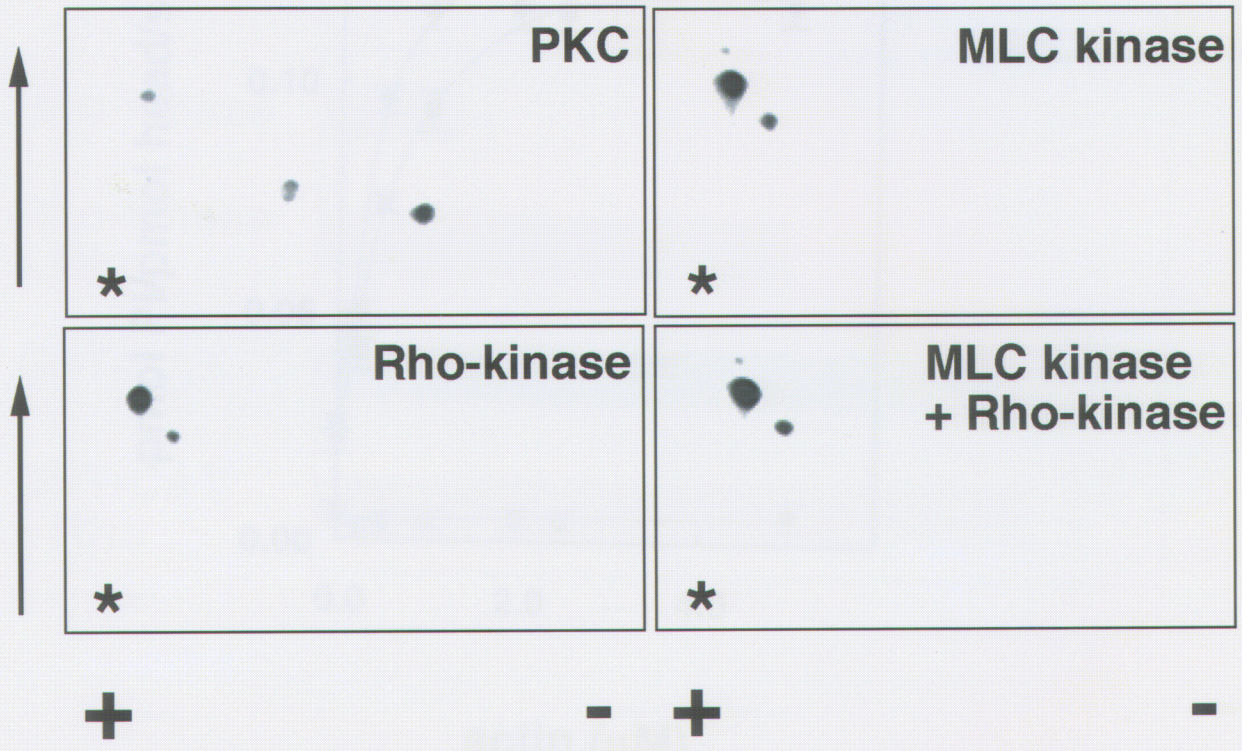

Fig. 14

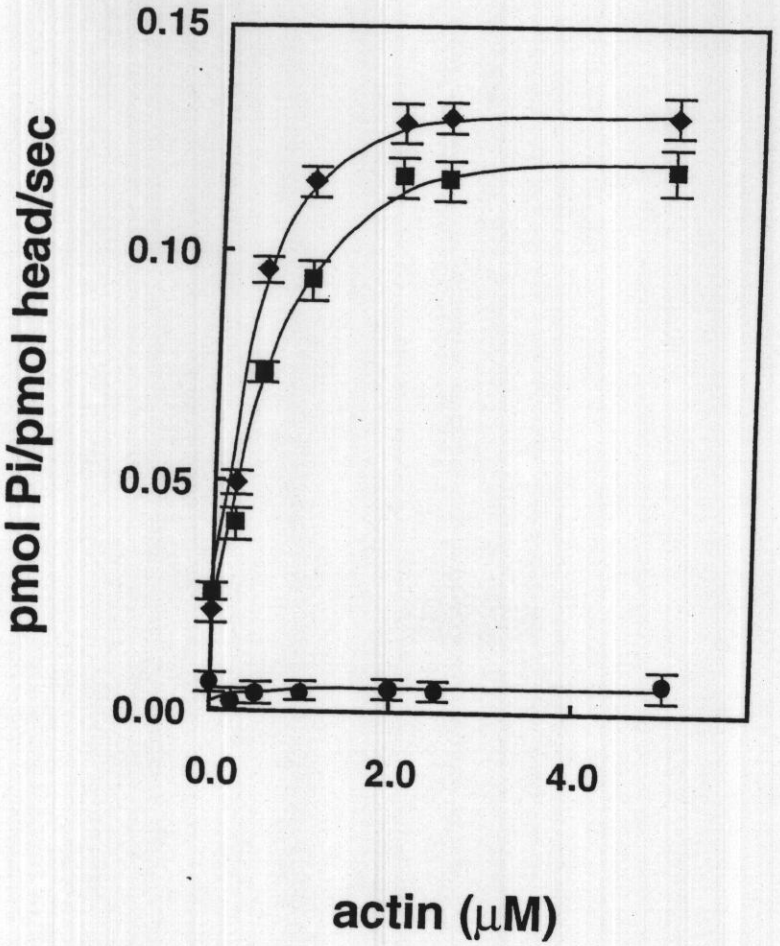

Fig. 15

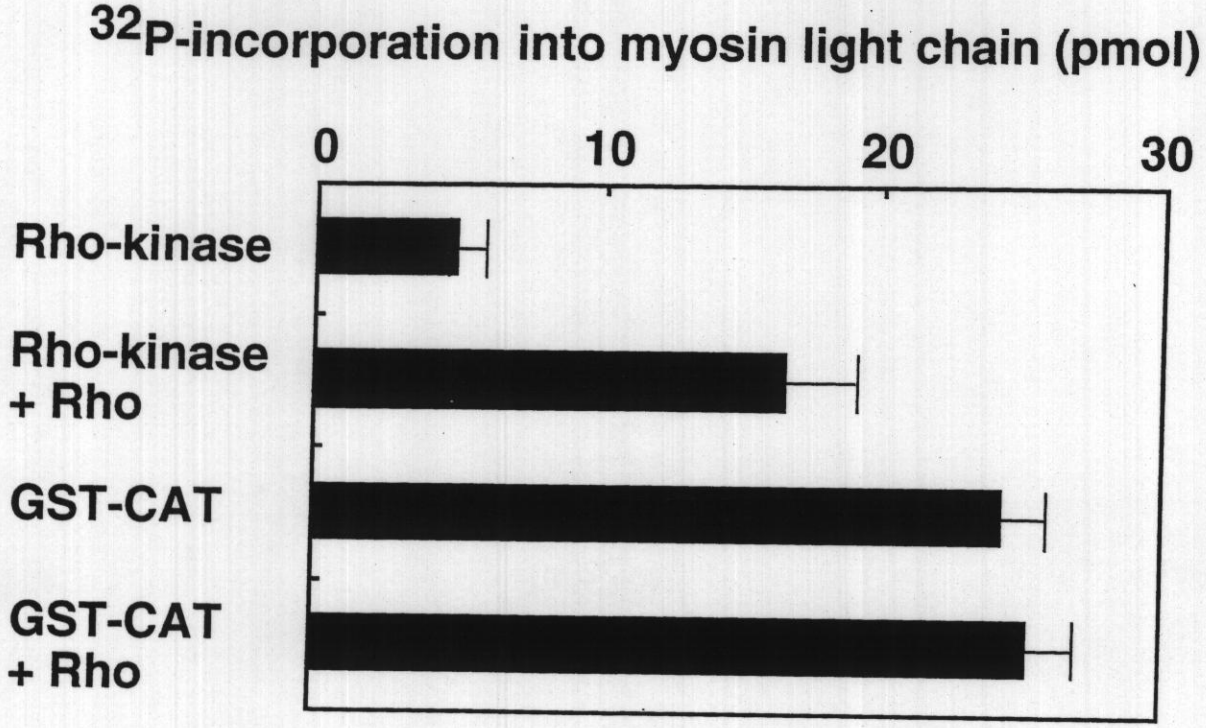
^{32}P-incorporation into myosin light chain (pmol)
0
10
20
30
Rho-kinase
Rho-kinase + Rho
GST-CAT
GST-CAT + Rho

Fig. 16

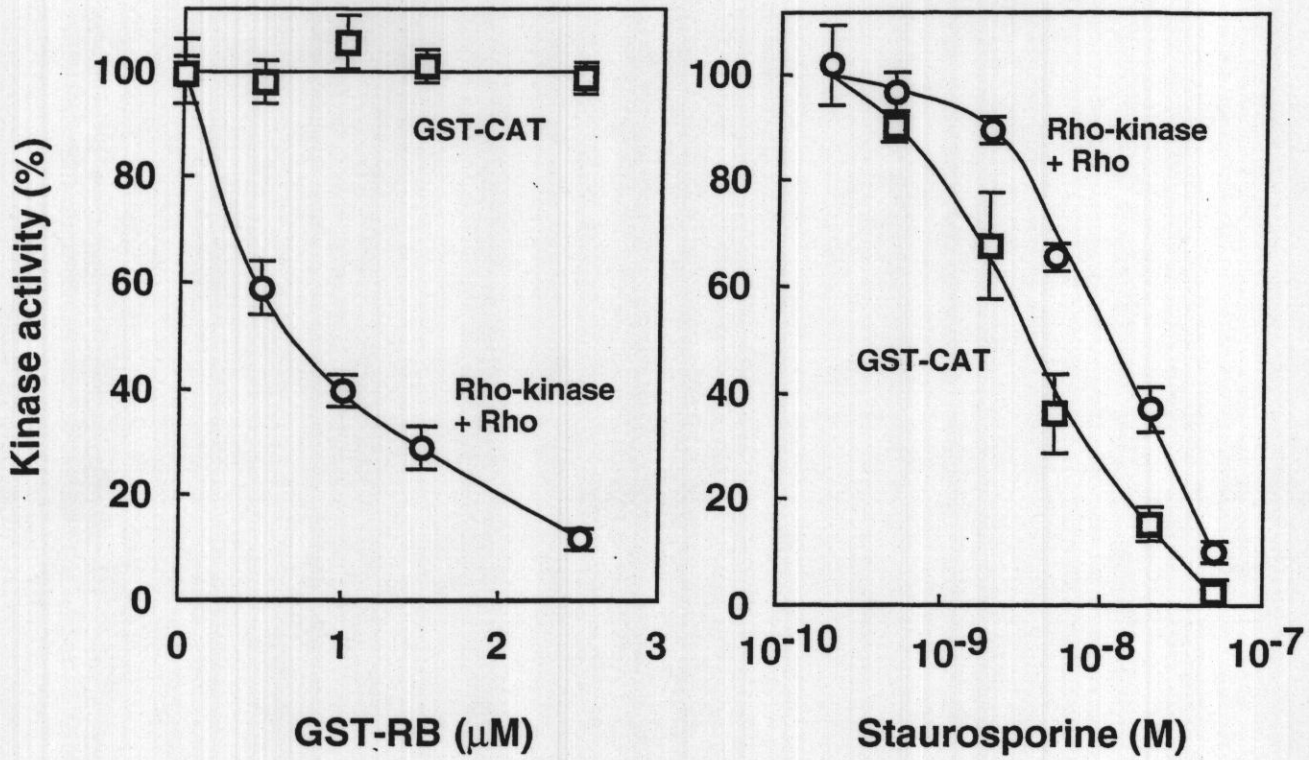
Kinase activity (%)
100
80
60
40
20
0
GST-CAT
Rho-kinase
+ Rho
0
1
2
3
GST-RB (μM)
100
80
60
40
20
0
Rho-kinase
+ Rho
GST-CAT
10-10
10-9
10-8
10-7
Staurosporine (M)

Fig. 17

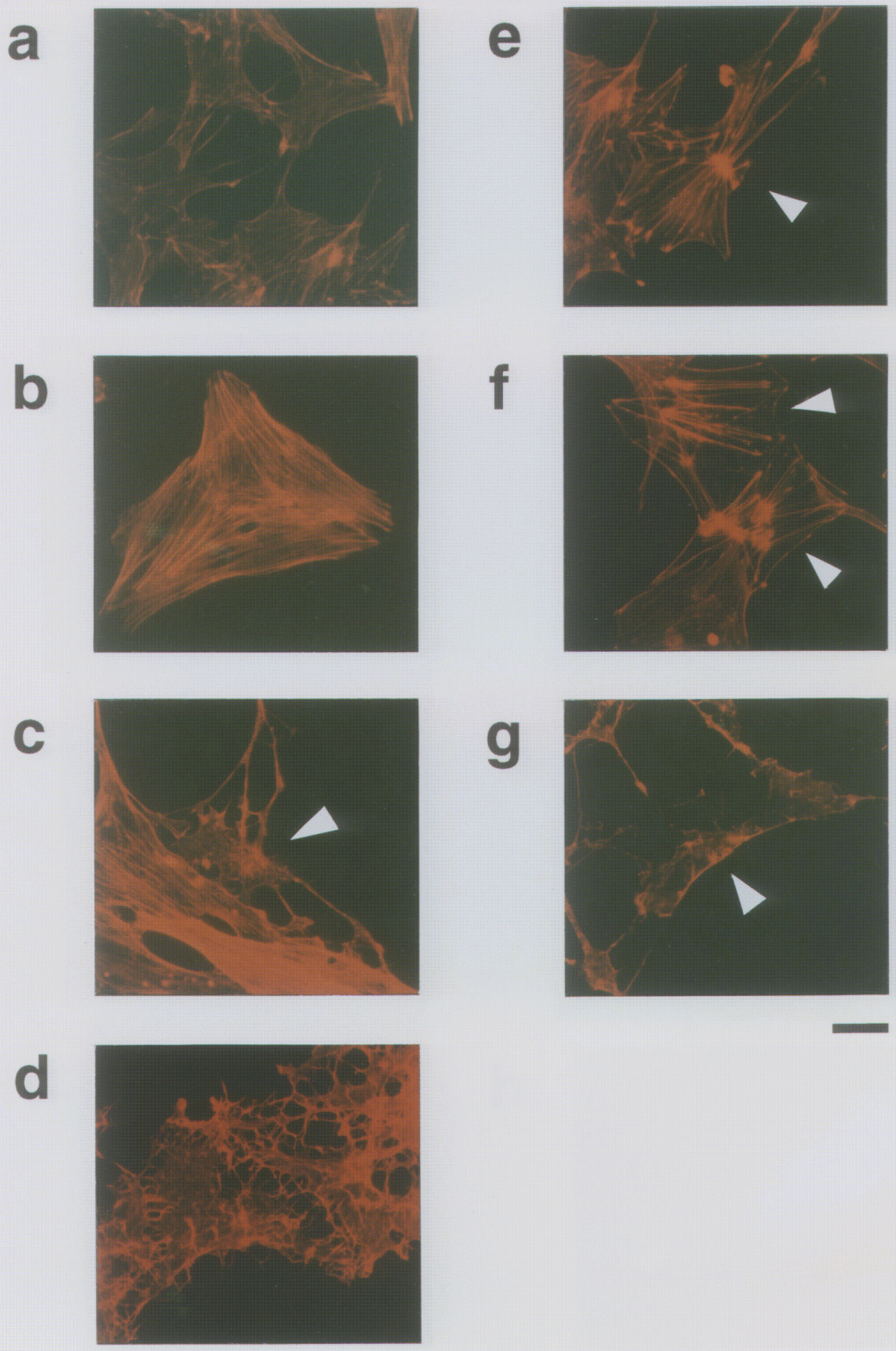

Fig. 18

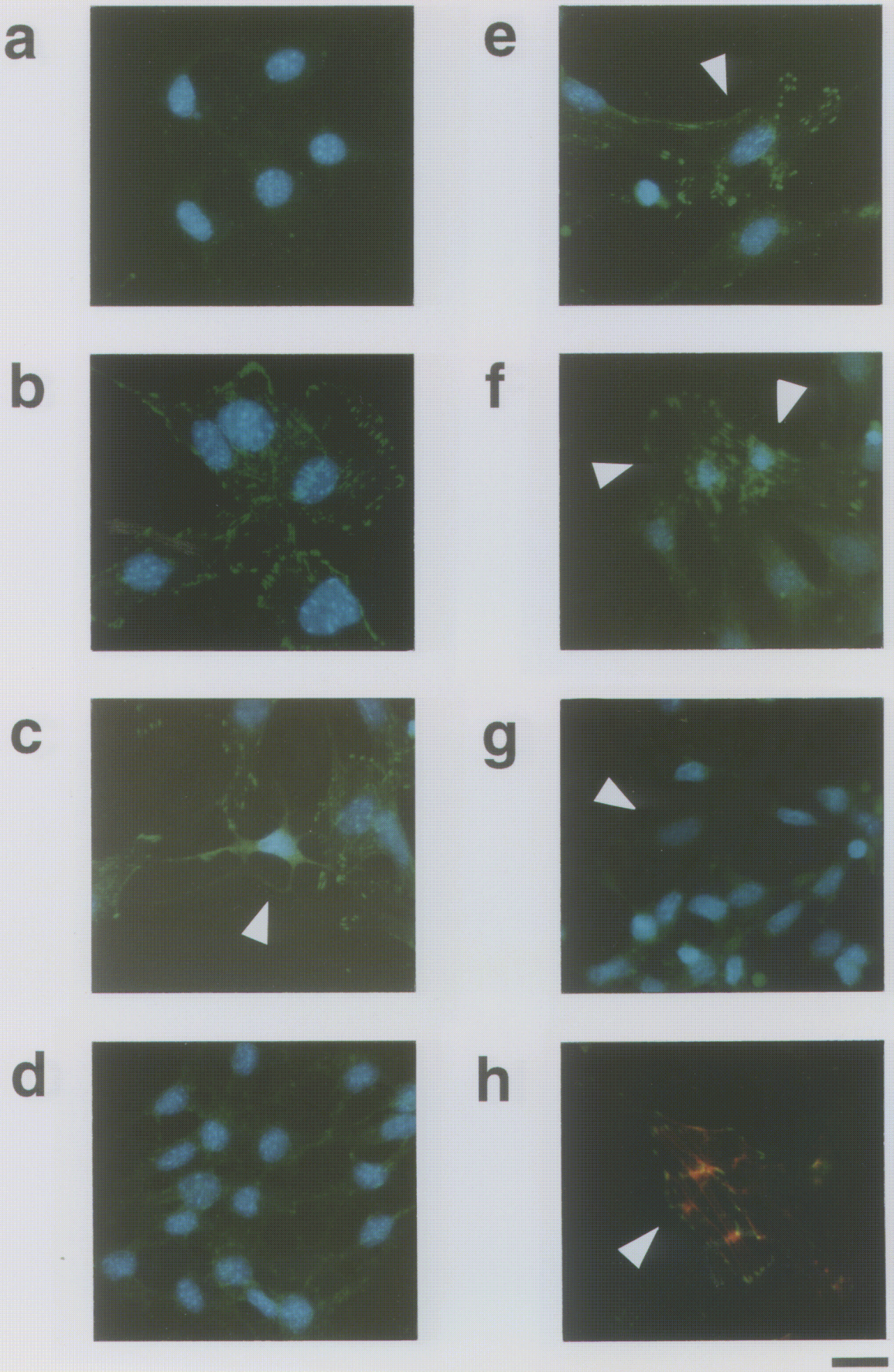

Fig. 19

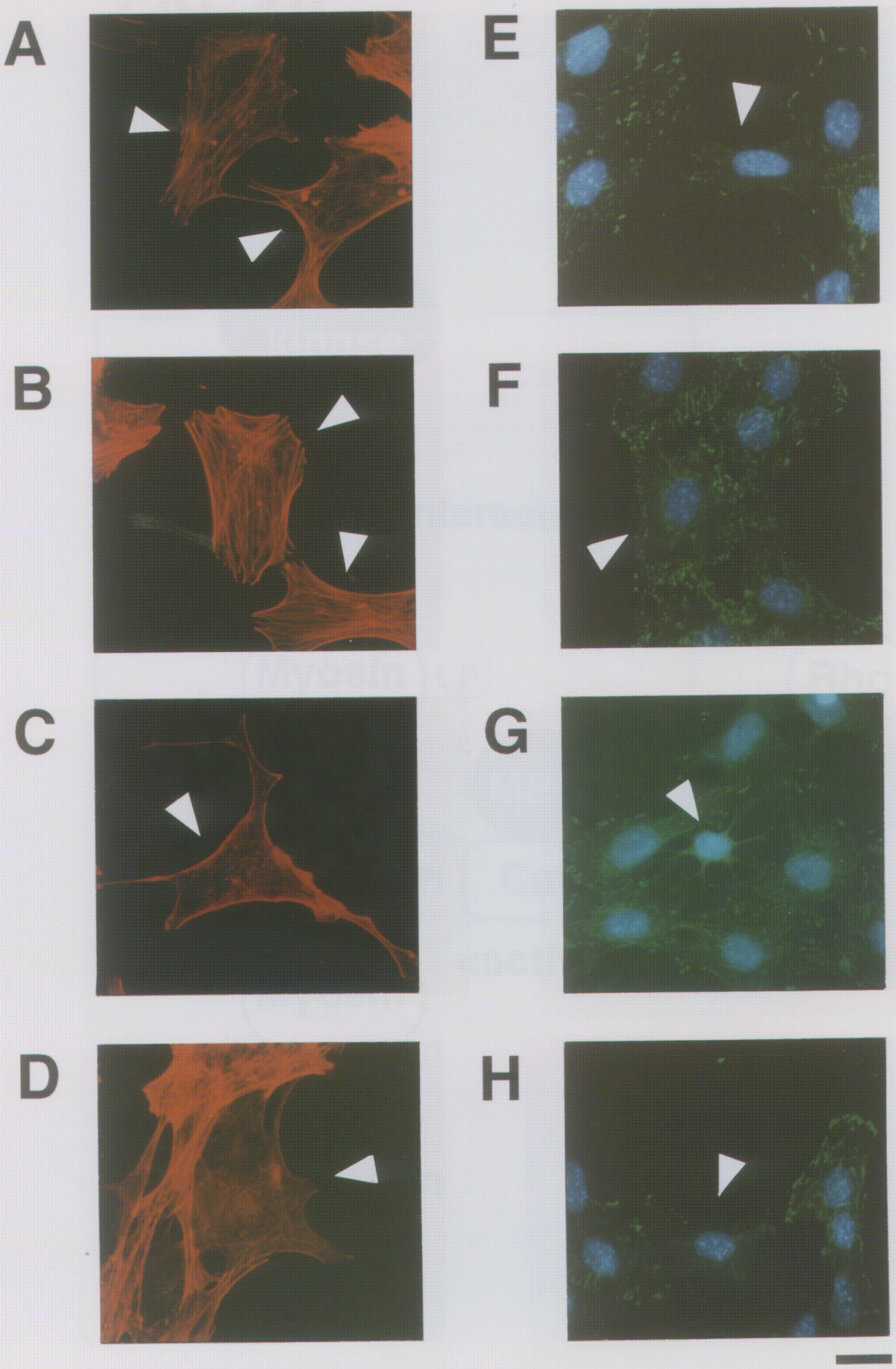

Fig. 20

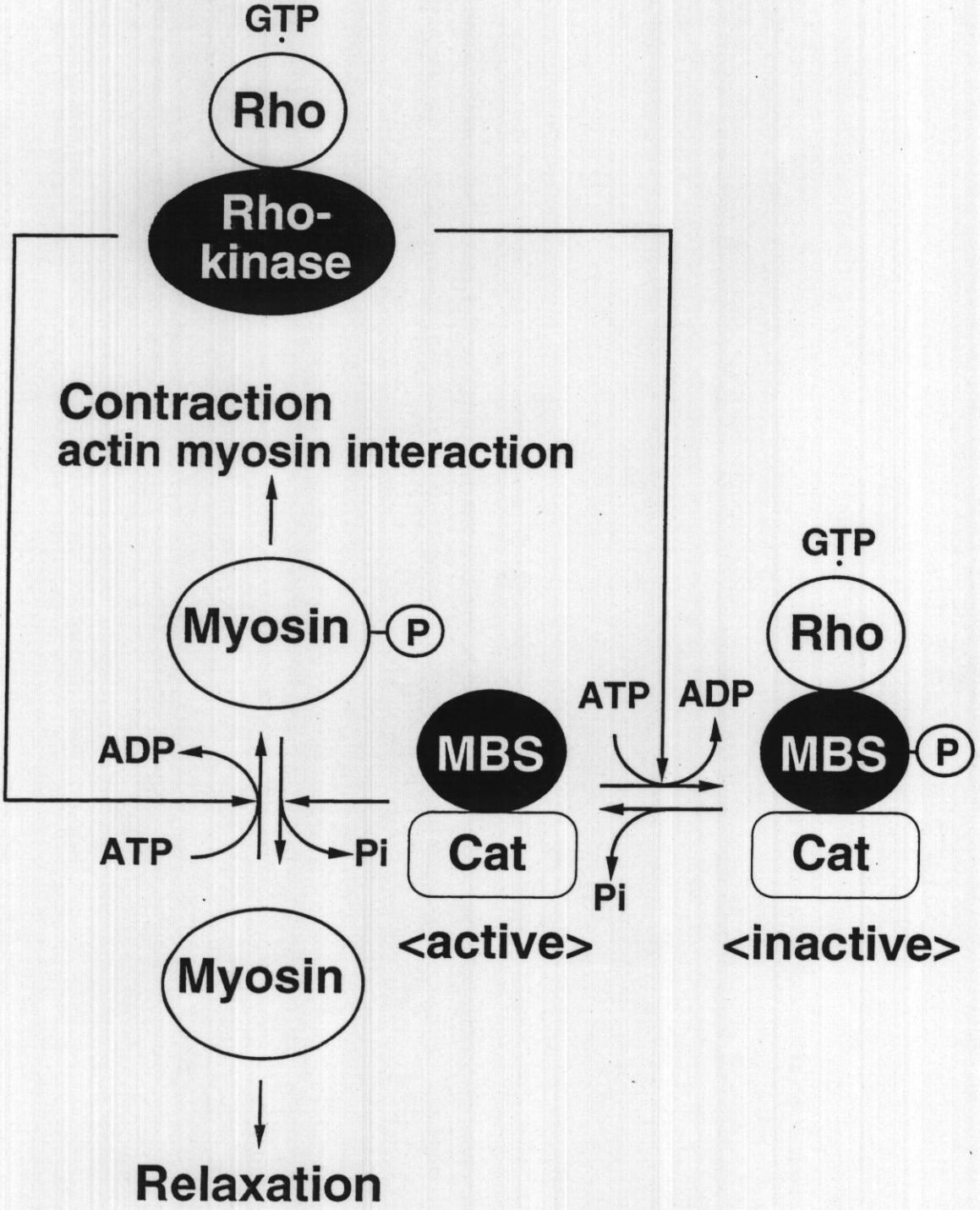
GTP
Rho
Rho-
kinase
Contraction
actin myosin interaction
Myosin
P
ADP
ATP
Pi
Myosin
Relaxation
GTP
Rho
ATP
ADP
MBS
MBS
P
Cat
Cat
Pi
<active>
<inactive>

Publication list; Mutsuki Amano

1. Chihara, K., **Amano, M.**, Nakamura, N., Yano, T., Shibata, M., Tokui, T., Ichikawa, H., Ikebe, R., Ikebe, M., and Kaibuchi, K. (1997)
Cytoskeletal rearrangements and transcriptional activation of c-fos serum response element by Rho-kinase.
J Biol Chem **272**, 26121-25127

2. Kureishi, Y., Kobayashi, S., **Amano, M.**, Kimura, K. Kanaide, H., Nakano, T., Kaibuchi, K., Ito, M. (1997)
Rho-associated kinase directly induces smooth muscle contraction through myosin light chain phosphorylation.
J Biol Chem 272, 12257-12260

3. Kosako, H., **Amano, M.**, Yanagida, M., Tanabe, K., Nishi, Y., Kaibuchi, K., Inagaki, M. (1997)
Phosphorylation of glial fibrillary acidic protein at the same sites by cleavage furrow kinase and Rho-associated kinase.
J Biol Chem **272**, 10333-10336

4. **Amano, M.**, Chihara, K., Kimura, K., Fukata, Y., Nakamura, N., Matsuura, Y., and Kaibuchi, K. (1997)
Formation of actin stress fibers and focal adhesions enhanced by Rho-kinase.
Science **275**, 1308-1311

5. **Amano, M.**, Ito, M., Kimura, K., Fukata, Y., Chihara, K., Nakano, T., Matsuura, Y., and Kaibuchi, K. (1996)
Phosphorylation and activation of myosin by Rho-associated kinase (Rho-kinase).
J Biol Chem **271**, 20246-20249

6. Kimura, K., Ito, M., **Amano, M.**, Chihara, K., Fukata, Y., Nakafuku, M., Yamamori, B., Feng, J., Nakano, T., Okawa, K., Iwamatsu, A., and Kaibuchi, K. (1996)
Regulation of myosin phosphatase by Rho and Rho-associated kinase (Rho-kinase).
Science **273**, 245-248

7. Matsui, T., **Amano, M.**, Yamamoto, T., Chihara, K., Nakafuku, M., Ito, M., Nakano, T., Okawa, K., Iwamatsu, A., and Kaibuchi, K. (1996)
Rho-associated kinase, a novel serine/threonine kinase, as a putative target for the small GTP-binding protein Rho.
EMBO J **15**, 2208-2216

8. **Amano, M.**, Mukai, H., Ono, Y., Chihara, K., Matsui, T., Hamajima, Y., Okawa, K., Iwamatsu, A., Kaibuchi, K. (1996)
Identification of a putative target for Rho as a serine-threonine kinase protein kinase N.
Science **271**, 648-650